Statistical Model for Spot Fire Hazard

Prepared by A. MURASZEW and J. B. FEDELE
Vehicle Engineering Division
Engineering Science Operations

20 December 1976

Prepared for

RIVERSIDE FOREST FIRE LABORATORY
PACIFIC SOUTHWEST FOREST AND RANGE EXPERIMENT STATION
UNITED STATES DEPARTMENT OF AGRICULTURE - FOREST SERVICE
DESIGNATED STATION REPRESENTATIVE: R. CHASE

PSW Grant No. 22

THE AEROSPACE CORPORATION

Aerospace Report No.
ATR-77(7588)-1

STATISTICAL MODEL FOR SPOT FIRE HAZARD

Prepared by

A. Muraszew and J. B. Fedele
Vehicle Engineering Division

20 December 1976

Engineering Science Operations
THE AEROSPACE CORPORATION
El Segundo, Calif. 90245

Prepared for

Riverside Forest Fire Laboratory
Pacific Southwest Forest and Range Experiment Station
United States Department of Agriculture - Forest Service
Designated Station Representative: R. Chase

PSW Grant No. 22

STATISTICAL MODEL FOR SPOT FIRE HAZARD

Approved by

A. Muraszew, Senior Staff Engineer
Aero Engineering Subdivision

E. G. Hertler, Director
Aero Engineering Subdivision
Vehicle Engineering Division
Engineering Science Operations

P. M. Stevens, Director
Resources Development Office
Energy and Transportation Division
Civil Operations

CONTENTS

CONTENTS (Continued)

TABLES

FIGURES

NOMENCLATURE

a	fire whirl core radius
a_o	fire whirl core radius at core base (at $z = 0$)
A	drag area of a firebrand in its maximum drag orientation
A_g	convection column ground width (normal to fire front)
b	convection column half-width
b_o	convection column half-width at the high and low buoyancy zone interface (at $z = \ell$)
b_g	column half-width at the ground ($2b_g = A_g$)
C_D	firebrand drag coefficient in its maximum drag orientation
C_r	radiation loss factor
$\overline{d}$	mean diameter of dead fuel
$\overline{d}_a$	mean diameter of all fuel
D	instantaneous firebrand diameter
D_{imp}	firebrand diameter at impact
D_o	initial firebrand diameter
F_d	firebrand generation function for a firebrand with diameter d (within that size class)
g	gravitational acceleration constant
h_{cr}	maximum distance between two spot fires over which rapid coalescence can occur
H	firebrand thickness
H_c	fuel heat of combustion
K	fuel-dependent parameter in the equation for F_d [Eq. (21)]
L	firebrand length

L_{max}	maximum travel distance for a given firebrand size for which $\rho_{imp} \geq \rho_{cr}$.
L_1	distance within which the main fire front will overtake any ignition point before a spot fire can start spreading
L_3	maximum threat distance (greatest L_{max}) of all sizes of viable firebrands
ℓ	height of the convection column high buoyancy zone
ℓ_{x_d}	maximum distance a firebrand of size d can travel and land without burning up in flight
m	mass of a firebrand
M	fuel or firebrand moisture content, in percent
$\dot{M}_f$	mass burn rate of the fuel within a fire whirl
N_d	potential number of firebrands of size class of diameter d which could be lifted by a convection column per unit length of fire front per second
$N_{d, \gamma_{1,2}}$	potential number of firebrands of size class d, which have an initial position between γ_1 and γ_2 (r_1 and r_2)
$N_{s_{d, \gamma_{1,2}}}$	expected number of spot fires due to the $N_{d, \gamma_{1,2}}$ firebrands
P(n) or $P(n;\lambda)$	probability of having n spot fires when the mean or expected number is λ
$P[\geq Y]$ or $P[\geq Y; A, t]$	probability of coalescence of at least Y spot fires anywhere within an area A and time t
P_{ig}	probability of the recipient fuel being ignited by a firebrand
P_{ig_o}	ignition probability as determined by the National Fire-Danger Rating System (Table 1)
P_r^*	Prandtl number evaluated at the mean temperature between the fuel surface and the fire whirl core

NOMENCLATURE (Continued)

Q_c	effective heat of combustion, including radiation losses and the energy required to pyrolyze the fuel
Q_i	effective fuel heat of ignition
R	fuel linear burn rate (fire front spread rate)
R_o	fire front spread rate in the absence of wind or ground slope
R'	linear burn rate of fuel within a fire whirl, ft/sec
t_c	firebrand flight time within convection column
t_t	total firebrand flight time
t_w	firebrand in-wind flight time (in-flight burning time)
t_L	fire whirl lifetime
$\bar{t}_{fl}$	typical firebrand time of flight to travel a distance of L_1
$\bar{t}_{ign}$	mean dead fuel ignition time, flaming combustion [Eq. (3)]
$\bar{t}_{ign,n}$	mean dead fuel ignition time, glowing combustion [Eq. (30)]
t_{res}	on-ground burning time of a firebrand
t_{resid}	burnout time (on-ground) for the average size fuel member (mean of dead and live fuel) with the average moisture content
$\bar{t}_{spr}$	on-ground burnout time of the average dead fuel
T	gas temperature, fire whirl mean core temperature
T_s	burning fuel surface temperature
T_∞	ambient air temperature
u	gas vertical velocity
u_o	fire whirl vertical gas velocity at core base; convection column vertical gas velocity

NOMENCLATURE (Continued)

V_{cr}	firebrand fall velocity within column or fire whirl
W	fire whirl gas azimuthal velocity
W_f	instantaneous firebrand fall velocity
W_{f_o}	initial firebrand fall velocity
W_x	x-component of the wind velocity
W_z	vertical wind velocity component
ΔW_d	dead fuel weight per unit area of size class d
x	horizontal coordinate in the direction of the horizontal wind velocity component
$\bar{x}$	mean distance traveled by a firebrand which is lifted by a fire whirl
$\bar{x}_{max}$	maximum mean distance traveled by a firebrand
Y	number of spot fires required to coalesce
z	vertical coordinate
z_e	vertical extent of fire whirl and its initiating external circulation
β	fuel packing ratio
β_{op}	optimum packing ratio for maximum fire spread rate
γ	ratio of initial firebrand radial position in fire whirl to fire whirl core base radius
Γ	circulation intensity of external circulation (ft^2/sec)
λ	expected or mean number of spot fires
ϕ	convection column centerline tilt angle due to wind, measured from the vertical
υ_∞	ambient air kinematic viscosity

NOMENCLATURE (Concluded)

ρ	instantaneous firebrand density
ρ_b	fuel bulk density
ρ_c	firebrand burnout, or char, density
ρ_{cr}	firebrand critical impact density (a firebrand is not an ignition threat if $\rho_{imp} < \rho_{cr}$)
ρ_{imp}	firebrand impact density
ρ_{fl}	convection column high buoyancy zone density
ρ_ℓ	convection column low buoyancy zone density
ρ_w	fire whirl mean gas density
ρ_o	initial firebrand density
τ_{res}	residence time within the convection column of the mean size fuel element
θ	azimuthal coordinate of firebrand within fire whirl and swirl environment

I. INTRODUCTION

In some intense wildfires the difficulty of fire control is augmented by the spot fires initiated by firebrands. In urban fires flames are often propagated into residential areas by firebrands landing on wood shake roofs, starting a conflagration.

In some cases, such as the Sundance fire (Rothermel [1967], Anderson [1968]) or Australian fires (Cheney and Bary [1969], firebrands have flown over distances of several miles initiating distant spot fires and secondary fire fronts. It is known that men have perished and equipment has been destroyed because of the unexpected secondary fire front encircling the fire fighters.

The need for understanding and predicting firebrand formation and behavior was the motivation for studies started at The Aerospace Corporation several years ago. While several researchers whose work was reviewed by A. Muraszew [1974] investigated the firebrand problem, no comprehensive theory or model was available for predicting firebrand-generated spot fires.

The problem is quite complex in that it involves (a) the characterization of convection columns or fire whirls formed over the fire front, (b) the characterization of fuels as firebrand donors, (c) the assessment of the probability of firebrand generation and lifting by the column, (d) the calculation of firebrand trajectories, and (e) the assessment of the probability of recipient fuel ignition and fire spreading.

The work on the problem was started at The Aerospace Corporation in 1972 and consisted of a review of the existing literature on firebrands, characterization of a two-dimensional thermal convection column based on the previous work of other investigators, and experimental work on firebrand burning in still air. This work was described by Muraszew [1974].

It appeared from the characterization of the convection column that even in case of large fires, like the California Romero fire in 1971, the uplift velocities in such a column were not high enough to lift large firebrands; hence, any firebrands produced with such columns will be small. Such small embers, emitted from the fire front, will fall a short distance (from zero to several hundred feet) from the fire front. If several embers fall close together, each initiating a spot fire, the spot fire may coalesce into a secondary fire front "jumping" ahead of the main fire. Therefore, it is not sufficient to estimate the probable number of spot fires; it is also necessary to define criteria for spot fire coalescence and probability of occurrence.

The inception of long-range spot fires required a more powerful firebrand lifting mechanism, such as the relatively short-lived fire whirl. It should be realized that a fire whirl can generate firebrands that may land anywhere from the fire front to a certain maximum distance. The term "long-range firebrands" reflects the fact that the maximum distance can be quite large and can amount to several miles. It should be also realized that between the two firebrand lifting mechanisms described above there may be other special cases (crown fires, canyon fires, fire storms) which may result in an "intermediate" range firebrand. Such cases were not considered in the analyses because of the unknown and undefined phenomenology associated with them.

The investigation of fire whirls [both analytical at The Aerospace Corporation and experimental at the University of California, Santa Barbara (UCSB)] was started in 1974 under the funding of the U. S. Department of Agriculture (USDA) Forest Service, Intermountain Forest and Range Experiment Station, Northern Forest Fire Laboratory (NFFL) in Missoula, Montana, with technical supervision by R. C. Rothermel. The work continued under a subsequent grant from the NFFL in 1975 and culminated in establishing a mathematical model of a fire whirl verified by the experimental data. Scaled up equations for actual fire whirl characterization

subject to field verification were also obtained, enabling calculation of firebrand trajectories within and outside of a fire whirl.

Parallel with this work an experimental program on the rate of firebrand burning in wind was initiated and carried out by R. C. Rothermel in the NFFL. From this work, semi-empirical formulas were defined describing the rate of average density change of a firebrand as a function of its initial size, wind velocity, moisture content, and time. Using these formulas together with an experimentally derived relationship on firebrand fall velocity by Tarifa [1967] and combining it with fire whirl calculated uplift velocities, it was indeed confirmed that firebrands could travel even with a moderate wind of 20 mph to distances over two miles and still have sufficient mass left at impact to initiate a spot fire. The firebrand burning and fire whirl characterization work is described in two reports by Muraszew, Fedele, Kuby [1975 and 1976].

With the above work in hand, we are now in the position to develop a model for the prediction of the probability of spot fire initiation and spreading for short-range firebrands from conventional convection columns and long-range firebrands created by the more powerful mechanism of a fire whirl. It is also useful to know the range of firebrands and the potential for recipient fuel ignition in order to define the safe width of a fuel break which would contain the short-range firebrand hazard. These aspects are analyzed in this report.

In the case of long-range firebrands it is impossible to consider any fuel breaks because of the distances involved. The hazard of such firebrands can be mitigated in some cases, once their probable location and spot fire probability are known, by measures preventing an easy ignition of recipient fuels. In many cases, all that it may be possible to do is to evacuate the threatened area if lives are endangered.

It was recognized that, whatever statistical model for spot fires is developed, such a model will include some unknown empirical constants that will have to be quantified later by field observations. It should also be kept in mind that while the firebrand model is developed for wildfires it could be used with modifications to predict the hazard of spot fires in urban or suburban fires. The work on the statistical model reported here was funded by the USDA Forest Service, Pacific Southwest Forest and Range Experimental Station, Riverside, California, under the direction of C. W. Philpot.

Following verification of the spot fire model, the tasks remaining to be done in the future on firebrands are to develop a model for the initiation of fire whirls and to integrate the statistical model into the general Fire Spread Model under development by Pacific Southwest Research Work Unit 210.

The Fire Spread Model will ultimately be able to predict the continuous progress of a fire front as well as assess and predict the hazard and location of spot fires and spot fire coalescence into a secondary fire front. If this is done on a real-time basis, it will provide the fire managers with a powerful and modern tool for an efficient and safe way of fire fighting.

II. OBJECTIVES

The primary objective of this study is the establishment of a physical approach and formulation of a statistical model for prediction of the short- and long-range spot fire hazard. A basic goal of this study as in the previous work of the authors is to generate a model which would utilize fuel or weather input data usually available to fire managers. Subgoals are the following:

a. Definition of fuel break widths which would contain the short-range firebrand hazard

b. Definition of criteria for spot fire probability of occurrence and for coalescence

c. Recommendations of future activity to validate the analytical models and further define the mechanisms involved in initiation of fire whirls.

III. SHORT-RANGE SPOT FIRES

A. APPROACH

To obtain a probability of spot fires generated by firebrands lofted by a convection column existing over a fire front, the following analytical steps were taken:

a. The convection column was characterized.

b. Trajectories of firebrands and their condition at impact were calculated for various sizes of firebrands.

c. The potential number of firebrands available of various sizes per unit of time was calculated from the burning fuel characteristics.

d. The firebrand generation function was assumed.

e. The number of firebrands impacting at various distances from the fire front was calculated.

f. The probability of ignition of recipient fuel by impacting firebrands was determined.

g. The expected number of firebrand-caused ignition points as a function of time per unit length of the fire front and their relative importance on fire behavior was determined.

h. The probability of spot fire occurrence at various distances and time intervals was calculated.

A brief description of the approach taken in each of the steps will be given to provide the reader with a quick overview of the methodology adopted by the authors. A flow diagram illustrating these steps is given in Appendix A.

The convection column was characterized on the basis of work performed earlier by other investigators and summarized by Muraszew [1974]. The main input to that characterization is the fire spread rate and ambient wind. The main output is the convection column shape and uplift velocity.

Firebrand trajectories were calculated based on earlier work by Tarifa [1967] and Young [1973], for given properties of the ambient wind. Firebrand mass and size at impact were calculated using semi-empirical

equations obtained from experimental in-wind burning data reported by Muraszew, Fedele, Kuby [1976]. This calculation permitted elimination of those firebrands which, while still burning at impact, had too little mass left to be able to ignite the recipient fuel. Thus, the trajectory calculation gave the distances at ground impact and the remaining mass of firebrands as a function of their initial size, density, and location in the convection column. Calculations showed that the impact distance varied approximately linearly with the initial location of the firebrand in the convection column. Since this initial location is random and there is an equal chance of a firebrand being either at the edge of the column or in its middle, an even distribution of firebrands of given initial size across the impact distance was assumed.

In calculation of the potential number of firebrands of a given size it was assumed that only dead fuel with low moisture content will provide firebrands which would likely continue to burn in the air after leaving the convection column. Consequently, the data on the amount of the dead fuel as a fraction of total burning fuel loading is needed such, for instance, as reported for chaparral by Rothermel and Philpot [1973]. Also, the size distribution of the dead fuel is required such, for instance, as reported for chamise by Countryman and Philpot [1970]. With that information available, and assuming some average ratio of firebrand length/diameter, the number of potential firebrands in a given size interval can be calculated.

Of course, not all of the potential firebrands will be lifted. The convection column uplift velocity will limit the maximum size of "liftable" firebrands. There is also some statistical function (firebrand generation function) which will depend on the fuel type, fuel configuration, gas velocity, etc., and which will determine the probable fraction of potential firebrands that could be lifted. To obtain the probable rate of firebrands lifted, the probable number has to be divided by the time period during which the fire sweeps through a width equal to the convection column width at ground level.

The firebrand generation function that will define the probable fraction of firebrands lifted is an unknown parameter for which no field observation or experimental data are available. Consequently, a function was assumed based on the ratio of convection column uplift velocity to the gas velocity required to lift firebrands (of given size) and containing a single experimental constant which was parametrically varied in this report; the constant will need field observation data for various fuel types for evaluation in the future.

From the calculation of the probable number of firebrands lifted and of the distance they can travel as a function of their initial size and location in the column, and with a uniform distribution across that distance, a number of firebrands of a given size impacting within a given time interval per unit of distance per unit width of the fire front can be calculated. From the in-flight burning behavior of firebrands (Muraszew, Fedele, Kuby [1976]), their mass at impact can also be determined. The density of the impacting firebrands will decrease progressively with increasing distance from the fire front. If a firebrand's impact mass is suffuciently large, it can burn on the ground for a sufficient length of time to cause recipient fuel ignition.

The probability of recipient fuel ignition is based on two sets of data: one is derived from a series of experiments carried out on in-wind burning of firebrands at the NFFL and the other is data in the USDA Forest Service National Fire-Danger Rating System. The NFFL experiments indicated that for short flight time the firebrands will be flaming at impact. Consequently, all firebrands above a certain critical mass at impact will have an equal random chance to ignite the recipient fuel. This random chance is determined from the National Fire-Danger Rating System which relates to the probability of ignition of fine fuels as a function of air temperature and fuel moisture. These ignition data do not recognize the effects of fuel loading (or packing ratio), the types of fine fuels, or other factors, although it was stated by Cheney and Bary [1969] that an optimum fuel loading for ignition does exist.

Considering this, the rate and number of ignition points is calculated by multiplying the rate and number of impacted firebrands at given distances by the National Fire-Danger Rating System ignition probability index multiplied by the fuel packing ratio factor. More experimental data is needed to verify and upgrade the ignition probability model.

It is realized that such "global" treatment of recipient fuel ignition may not represent actual conditions in that, for instance, fuel close to the fire front and heated by the flame radiation will be ignited much more readily than fuel farther away. Berlad [1970] distinguished between the danger of firebrands in relation to the recipient nonburning fuel temperature. If the temperature was at or above the spontaneous ignition point, then firebrands were of small significance since the fuel would ignite anyway. If, on the other hand, recipient fuel temperature was below the spontaneous ignition point, firebrands falling down in sufficient numbers could add significantly to the fire spread rate. However, firebrand-caused ignition points sufficiently close to the fire front are not a major source of concern for the spot fire problem, as explained in the following paragraph.

A determination of only the expected number of ignition points or spot fires is not sufficient. Equally important is the determination of the effect of spot fires on the fire front behavior and on the fuel break requirements. Let us consider the case of a burning firebrand leaving the convection column. The flight of a short-range firebrand will last for several seconds. After impact, assuming that ignition occurs, there will be several seconds ignition delay; following this, if a spot fire is formed, there will be a several-second delay before the flame starts spreading. During all this time the main fire front is advancing and the spot fires formed within a short and calculable distance from the fire front will be engulfed by the advancing flame and will have no great significance on the fire front behavior. At the other extreme of the distance from the fire front are firebrands which at impact are left with barely sufficient mass to ignite the recipient fuel. Any distance beyond

that is not of major concern because firebrands probably will have burned out in flight or are too small or light to burn long enough on the ground to ignite the recipient fuel. Thus, between the two extremes of the distances is the spot fire danger zone. If a fuel break can be provided whose width is equal to or greater than the travel distance of the barely ignitionable firebrands, the short-range firebrand and spot fire hazard is virtually elimiated. Unfortunately, this may not always be possible, because a vigorous fire front and convection column will enable the hazardous size firebrands to travel to distances beyond those that may be considered feasible for local fuel breaks, or because of strong wind which, even with moderate fires, can carry the firebrands to excessive-for-fuel break distances. In such cases, the hazard and danger of the spot fire zone is real. If the number of ignition points and subsequent spot fires in that zone is appreciable, a possibility of several spot fires occurring almost simultaneously may exist causing coalescence of those spot fires into a new fire front ahead of the main fire, thus resulting in a step-like increase in the fire spread rate or fire "jump."

The final step in the evaluation of the short-range firebrands is the definition of the probability of one or more spot fires occurring within a given area over a certain period of time, or of the probability of coalescence of spot fires into a new fire front. Taking the occurrence of a spot fire as a discrete random event (with the expected or mean rate of occurrence within a given area determined as described), then the occurrences of spot fires are described by a Poisson distribution by which the probability of a given number of spot fires occurring in a given time and area can be determined.

The remainder of Section III of the report will describe in more detail the key elements of the short-range spot fire hazard analysis. Examples of numerical application of the proposed method are given in Appendix C-I, II. One of the examples will represent an interval of the Romero fire in California in 1971, the other the case of burning logging slash with dead fuel loading of over 40 tons/acre.

B. FUEL CHARACTERISTICS AND RECIPIENT FUEL IGNITION

The fuel characteristics are germane to the firebrand problem from several aspects. The sizes and numbers of firebrands that are lifted up, burn, and travel away from the column depend on the characteristics of the burning fuel. The ignition of the recipient fuel by an impacting firebrand and the growth of an ignition point to a spot fire depend on fuel characteristics. The convection column (and fire whirl) properties also depend on various characteristics of the burning fuel.

1. FUEL PHYSICAL CHARACTERISTICS

The National Fire-Danger Rating System of 1974 recognizes five classes of fuel with respect to fuel size which could be ignited and consumed within the flaming front. Three classes are dead fuels of sizes (diameter or thickness) less than 0.25 in., between 0.25 in. and 1 in. and between 1 in. and 3 in. Since the fuel moisture is an important parameter in determining the ease of ignition and burning, the three size classes are also characterized by the response time to air humidity. The remaining two classes are live fuels: grass and other herbaceous plants, and twigs (less than 0.25 in. diameter) and foliage of woody plants. Woods of 0.25-in. size are considered to be the upper size limit of live fuels that can be dessicated and consumed within the flaming front.

To distinguish between the geographic areas of the country, the fuels are divided into nine fuel models (from models A through I) which define in general terms the amount of fuels present by class and its arrangement (i.e., ground litter, tree cover denseness, etc.). (The NFFL has recently categorized fuels into thirteen fuel models, which may be more realistic in their size class and loading characterization.)

It was assumed in our studies (and supported by experiments) that only dead fuels with moisture content below 20 percent are of a suitable material for firebrands. While it is appreciated that, in an established fire front,

dead fuels with higher moisture content may burn and even two classes of small size live fuels may be consumed, the fact remains that once such fuels are withdrawn from the fire front they will not support self-combustion and will extinguish quite rapidly. There also may be cases of special fuels such as excelsior which behave differently than normal dead or live fuels, but the present firebrand analysis must of necessity consider the normal fuel characteristics and cannot be detailed enough to consider a micro-case of special fuels.

In considering the fuel characteristics pertinent to firebrand formation in a given convection column, dead fuel size, moisture, and fuel arrangement are of primary importance. If a fuel is of approximately cylindrical shape, the size characteristic is defined by its diameter. If its shape is irregular, the characteristic size is proportional to the volume/surface ratio. Fuel size and density will define the limiting class of firebrand that can be lifted, the range of the firebrand discharged from the column, and the rate of its burning. Fuel moisture will determine the ease of firebrand ignition and will also have an effect on the burning rate during flight and after impact. Fuel arrangement, i.e., height of the fuel and dead fuel location and attachment, depth of the ground slash or litter, ground coverage, etc., will determine the value of the firebrand generation function or the number of firebrands actually lifted.

In determining the potential number of firebrands, the fraction of dead fuel and its size distribution must be known. The fraction of dead fuel will be a function of fuel age and some data on this are available. For instance, Figure 1 from Rothermel and Philpot [1973] shows the total fuel loading and the dead fuel fraction for chaparral. In case of logging slash left on the ground for sufficient time to reduce the fuel moisture, all fuel in the classes of interest (up to 3-in. size) can be considered firebrand material. From the usually available data on fuel loading (tons/acre), fuel age and known or assumed relationship of dead fuel fraction versus age, the dead fuel loading can be determined.

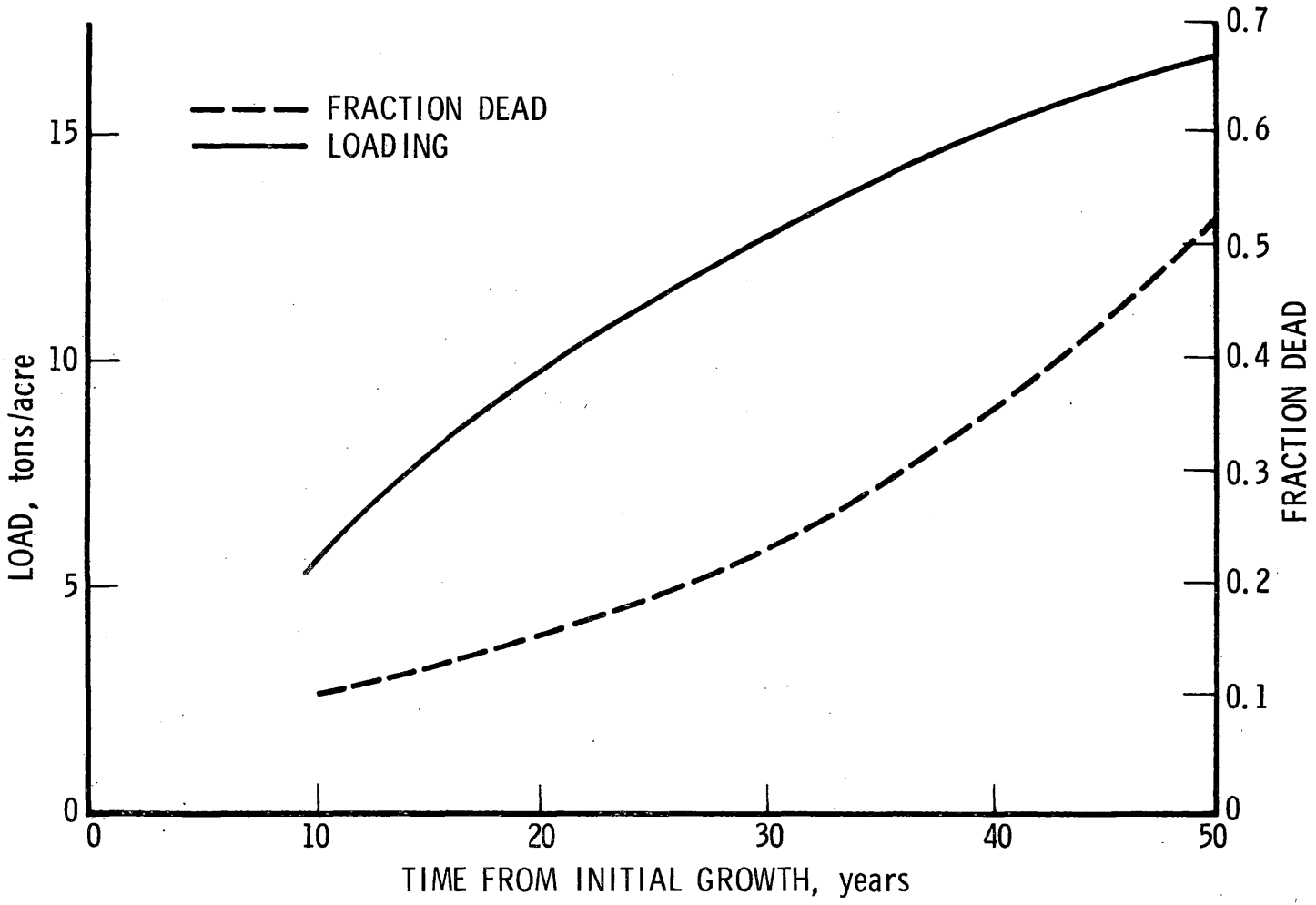

Figure 1. Chaparral Fuel Loading and Fraction Dead versus Age

To determine the potential number of firebrands, the size distribution of dead fuel must be known defining the fraction of mass, or volume for each of three or more fuel classes. Such a size distribution is shown in Figure 2 based on data from Countryman and Philpot [1970]. Within each size class, the cumulative weight distribution is taken to vary linearly with size. Assuming that for cylindrical dead fuel sticks an average length-to-diameter ratio of 10 is a reasonable value, then for a given group size interval from d_1 to $d_2 = d_1 + \Delta d$, the number of sticks can be calculated from

$$N_d = \frac{4 \Delta W_{d_{1,2}} R}{L \cdot \pi d_1^2 \cdot \rho_o} \qquad (1)$$

where

R	=	fire front spread rate
$\Delta W_{d_{1,2}}$	=	weight of dead fuel per unit area between diameter d_1 and d_2
L	=	stick length (assumed equal to $10 \cdot d_1$)
ρ_o	=	dead fuel density (initial firebrand density)
N_d	=	potential number of firebrands between d_1 and d_2 which could be lifted per second per unit length of fire front.

The spread rate R can be obtained from Rothermel's [1972] formulation. The inputs required for the calculation of R are wind speed, ground slope, and fuel characteristics such as size distribution, moisture content, fuel depth, packing ratio, etc. Many fire hazard areas have been or are in the process of being so characterized by the USDA Forest Service.

Equation (1) gives the mean rate at which firebrands within the size interval could be lifted per unit length of fire front, if all available fuel were lifted. To arrive at the probable number of firebrands within the size interval actually lifted, N_d is multiplied by a firebrand generation function (the fraction of all possible firebrands lifted) which is discussed in Section III-D.

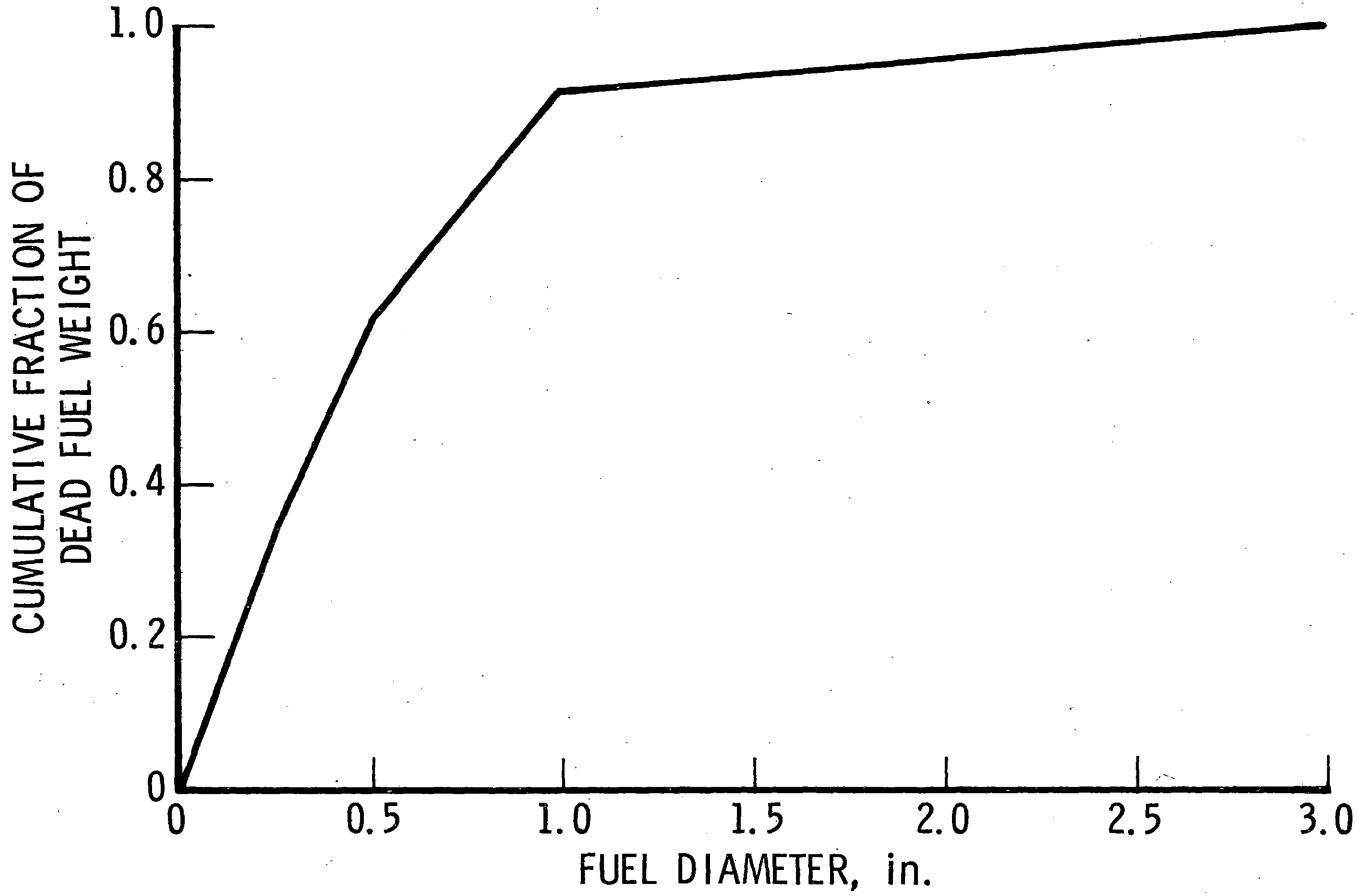

Figure 2. Cumulative Fraction Fuel Size Distribution of Chamise

2. RECIPIENT FUEL IGNITION: FIREBRAND BURNING CHARACTERISTICS

Another important aspect of fuel characteristics is the feasibility of its ignition by a firebrand. A great amount of research work was done in the past on piloted or radiative ignition of wood and some of this work was reviewed by Muraszew [1974].

For the short-range trajectories with a flight time of the order of 10 sec, the small firebrands (less than 0.25-in. diameter) will be most probably in a flaming stage. This statement is based on observations from NFFL experiments (Muraszew, Fedele, Kuby [1976]). Thus, the ignition of the recipient fuel (which is assumed to be initially at air temperature) will be of the pilot ignition type. The recipient fuel is heterogeneous and the fuel most likely to be ignited is the dead fuel. The ignition lag, i.e., time to ignite a fuel element, will depend on fuel type, on the ignition source heat flux, on the recipient dead fuel size, and on its moisture. It will be assumed here that the fuel element to be ignited by the firebrand is in or near the firebrand flame and, since all firebrands are assumed to be flaming on impact, the heat flux, if not its duration, is the same. Consequently, the ignition lag will be only a function of recipient fuel size and moisture. In defining some average ignition lag, this lag will be related to a mean size of the dead fuel expressed by

$$\bar{d} = \frac{4 \cdot \sum_{j=1}^{n} V_j}{\sum_{j=1}^{n} S_j} \qquad (2)$$

where V_j and S_j are the volume and surface area of a dead fuel "j" size class.

The ignition lag was discussed by Muraszew [1974] and from the data presented there an approximate formula for mean ignition lag for fuel sizes less than 2 cm (0.8 in.) is

$$\bar{t}_{ign} = 17.5 \cdot \bar{d}^{0.75} \left(\frac{M}{M_{ref}} \right)^{0.18} \tag{3}$$

where

$\bar{d}$ = mean dead fuel diameter, cm (< 2 cm)

M_{ref} = reference fuel moisture = 2 percent

M = fuel moisture, percent (< 20 percent)

$\bar{t}_{ign}$ = mean ignition lag, sec

In order for the recipient fuel to be ignited by a firebrand, the on-ground burning time of the firebrand should be equal to or greater than $\bar{t}_{ign}$. The on-ground firebrand burning time depends on the firebrand impact density and size, which in turn depend on the initial size and density of the firebrand and its in-flight burning characteristics.

Firebrand burning in wind was evaluated experimentally in the NFFL, and a semi-empirical formula was proposed by Muraszew, Fedele and Kuby [1976] defining the change in burning cylindrical firebrand average density

$$\frac{\rho}{\rho_o} = \exp\left(- \frac{t}{D_o^2 \cdot k} \right) \tag{4}$$

where

$k = 43.3 - 1.28 \cdot V + 0.022\, V^2$, sec/cm^2

t = burning time (from ignition), sec

D_o = initial firebrand diameter, cm

ρ = instantaneous firebrand average density

ρ_o = initial firebrand density

V = relative to wind firebrand velocity (equal to instantaneous fall velocity), mph.

For firebrands burning on the ground, a similar equation applies

$$\frac{\rho - \rho_c}{\rho_{imp} - \rho_c} = \exp\left(- \frac{t}{D_{imp}^2 \cdot 43.3}\right) \tag{5}$$

where

ρ_{imp} = firebrand density at impact

ρ_c = firebrand density at completion of burning

D_{imp} = firebrand diameter at impact, cm

The fuel does not burn completely, but some material in the form of char and/or virgin fuel will remain following completion of burning. For cylindrical firebrands, the density at completion of burning depends on its initial density and its diameter at impact, and is given by

$$\frac{\rho_c}{\rho_o} = 0.5\left(\frac{D_{imp}}{4}\right)^2 \tag{6}$$

This equation is valid for 5.25 cm > D_{imp} > 1.25 cm. For smaller than 1.25 cm diameter fuels, assume $\rho_c / \rho_o = 0.05$.

For practical determination of the firebrand on-ground burning time after impact, t_{res}, the final value of ρ in Eq. (5) was assumed to be 10 percent higher than ρ_c. For the sizes of firebrands found to be viable threats, the diameter changed little in the short flight time so that D_{imp} is taken to be D_o. (Similarly, for plate-like firebrands, the thickness changes little.)

From Eq. (4), ρ_{imp}/ρ_o can be obtained once the flight time is calculated from a trajectory computation as described in Section III-C, and the firebrand density at impact and the remaining on-ground burning time can be calculated as explained above from Eq. (5).

The effect of fuel moisture is incorporated into Eqs. (4) and (5) by modification of the exponential parameter k appearing in the equations. The equation for k given below Eq. (4) was for oven-dry fuel with nominal moisture content of 2 percent. Designating this value of k as $k_{(M=2)}$, then for a higher moisture content M

$$k_M = k_{(M=2)} \cdot \left(\frac{M}{M_{ref}}\right)^{0.44} \tag{7}$$

where M_{ref} = 2 percent.

A similar set of equations was presented by Muraszew, Fedele, Kuby [1976] for flat plates representing, for instance, bark pieces, leaf clusters, etc.

For a given size firebrand, from Eq. (5), there is a critical impact density for which the on-ground burning time (t_{res}) is equal to $\bar{t}_{ign}$. Firebrands of that size landing with a density greater than this critical value are viable candidates to ignite the recipient fuel. Firebrands landing with a smaller density are not ignition threats.

In addressing the problem of ignition probability by a viable firebrand, the type of recipient fuel is an important factor. For example, Bunting and Wright [1973] found that even glowing firebrands could easily ignite cow chips and punky wood if the fuel moisture was below 10 to 13 percent. Anderson and Stockstad [1973] found that rotten white fir samples with moisture content < 10 percent ignited very easily even with small glowing embers. Cheney and Bary [1969] stated that in Australian eucalyptus forests, under most wildfire conditions, flaming firebrands will have ignition probability approaching 1. Other fuels do not ignite so easily and require greater heat flux than that produced by small glowing embers. Unfortunately, consistent

ignition data on the ignitability of various fuels with a fixed glowing or flaming combustion source are not available to permit an analytical definition of fuel type effect, and assessment of ignition probability is reduced to the various observations made and their statistical interpretation.

Blackmarr [1972] performed ignition tests with a number of ignited matches dropped on the bed of slash pine litter with varying moisture content and observed the number of ignition points obtained as a percentage of the total number of ignited matches. The percentages were quite high and, even with a miniature match ($d \sim 0.2$ cm), approximately 40 percent of them ignited the pine slash at 20 percent moisture and 90 percent ignited at 15 percent moisture.

The National Fire-Danger Rating System [1974] provides a table related to fuel ignition probability which is common for all fine fuel types. The probability of ignition (by firebrands) is defined as a function of fuel moisture and dry bulb air temperature on either a sunny or a cloudy day. These data are reproduced in Table 1. It can be seen that the probability of ignition drops rapidly as fuel moisture increases and that, contrary to Blackmarr's data, there is practically no ignition at 20 percent fuel moisture. It is thought that the National Fire-Danger Rating System data represent the more realistic fuel arrangement found in nature (combination of live and dead fuels) than Blackmarr's uniform bed of slash pine litter; therefore, the former probability data were used in our analysis. Since the dead fuel is easier to ignite, the dead fuel moisture content is appropriate for Table 1. It is realized that these data do not include ignition variability with different fuel types, but until such data are obtained the existing data must suffice.

The ignition probability obtained from Table 1 is modified by applying a multiplicative packing ratio factor. Cheney and Bary [1969] found that the ignition probability decreased as the fuel packing ratio β decreased. For

Table 1. Ignition Component

Col. 10

State of Weather Col. 2		Fine Fuel Moisture (Percent) Col. 9															
Code 0-1	Code 2-9																
Dry Bulb Temperature (°F) Col. 3	Dry Bulb Temperature (°F) Col. 3	1	2	3	4	5	6	7 ↓ 8	9 ↓ 10	11 ↓ 12	13 ↓ 14	15 ↓ 16	17 ↓ 18	19 ↓ 21	22 ↓ 24	25 ↓ 25+
SUNNY	CLOUDY																
10→ 19	10→ 39	88	75	64	54	46	39	30	21	14	9	5	2	0	0	0
20→ 29	40→ 49	90	77	66	56	48	41	32	22	15	9	5	2	0	0	0
30→ 39	50→ 59	93	80	68	58	50	42	33	23	16	10	6	3	0	0	0
40→ 49	60→ 69	95	82	71	61	52	44	35	25	17	11	7	3	1	0	0
50→ 59	70→ 79	98	85	73	63	54	46	36	26	18	12	7	4	1	0	0
60→ 69	80→ 89	100	87	76	65	56	48	38	28	19	13	8	5	1	0	0
70→ 79	90→ 99	100	90	78	68	58	50	40	29	21	14	9	5	2	0	0
80→ 89	100→109	100	93	81	70	61	53	42	31	22	15	10	6	2	0	0
90→ 99	110→119	100	97	84	73	63	55	44	32	23	16	11	7	3	0	0
100→109	120→120+	100	100	87	76	66	57	46	34	25	18	12	8	4	0	0
110→119		100	100	90	79	69	60	49	36	27	19	13	9	4	1	0
120→120+		100	100	92	80	70	61	50	37	28	20	14	9	5	1	0

Purpose: To compute a number related to the probability that a fire will result if a firebrand is introduced into the fine fuel complex.*

Procedure: If the state of the weather is coded 2, 3, 4, 8, or 9 (column 2), or if the observation is being taken before 1000 or after 1500 LST, the dry-bulb temperature (column 3) is entered to the left in that section of the table labeled "cloudy." Otherwise, enter the temperature in the section labeled "sunny." Read the IC at the intersection of the column indexed by the FFM (column 9) and the row indexed by the dry-bulb temperature (column 3); record in column 10.

** If it is raining (state of weather code 5, 6, or 7) or there is snow or ice on the ground fuels, record a zero (0) in column 10.*

packing ratios greater than the optimum for maximum burning efficiency β_{op} the ignition probability is taken to be independent of the packing ratio so that

$$P_{ig} = P_{ig_o}(\beta/\beta_{op}) \quad \text{for } \beta < \beta_{op}$$

and (8)

$$P_{ig} = P_{ig_o} \quad \text{for } \beta \geq \beta_{op}$$

where P_{ig_o} is the value obtained from Table 1.

The possible existence of bare spots, i.e., spots not covered by fine fuels, can be taken into account by multiplying the ignition probability by the fraction of area covered by fine fuels. For simplicity, this fraction is taken as one in this report.

C. CONVECTION COLUMN AND FIREBRAND TRAJECTORY

The uplift force in a convection column is created by the thermal buoyancy of the air entrained in and heated by the burning fuel bed. The rate of fuel burning and hence the column velocity (and uplift force) are increased by increasing ambient wind speeds. Muraszew [1974] has reviewed past convection column investigations and has divided the convection column into a high buoyancy zone and a low buoyancy zone above it. Muraszew modeled the high buoyancy zone after Thomas [1962, 1965] and the low buoyancy zone after Morton [1956]. This modeling is summarized in the following paragraphs.

The high buoyancy zone contains the combustion reaction flame region and is characterized by a constant characteristic temperature and density. The vertical velocity increases to a maximum u_o at the upper end of the high buoyancy zone. The presence of intense turbulent gusts near the hot, burning fuel bed is expected to maintain a high level of velocity above the column

bottom. Consequently, the column uplift velocity is taken here to be constant and equal to u_o. The height of the high buoyancy zone (flame height) ℓ and u_o are functions of $\dot{M}_f$, the fuel burn rate per unit width of flame front. In cgs units

$$\ell = 400\ \dot{M}_f^{2/3}, \qquad u_o = 434\ \dot{M}_f^{2/3} \tag{9}$$

where

$$\dot{M}_f = R W_{n_t} \tag{10}$$

with W_{n_t} being the total fuel mass loading per unit area and R the fire front spread rate.

The high buoyancy zone characteristic temperature $T_{f\ell}$ is given by

$$27{,}200\ \rho_\infty \left[\frac{T_{f\ell} - T_\infty}{T_{f\ell}}\right]^{1/2} + 1 = \frac{H_c C_r}{C_{p_\infty}(T_{f\ell} - T_\infty)} \tag{11}$$

where H_c is the fuel heat of combustion ($\sim$8500 cal/gm) and C_r is the radiation loss factor ($\sim$0.95). Typically, $T_{f\ell} \sim 857^\circ$K. The density is obtained from

$$\rho_{f\ell} T_{f\ell} = \rho_\infty T_\infty \tag{12}$$

The convection column width at the ground A_g is assumed to be equal to the flame width which can be calculated according to Albini [1966] by

$$A_g = 2b_g = \tau_{res} R = \frac{\bar{d}_a^2}{4\alpha_{f_o}} R \tag{13}$$

where

b_g = half-width of the column at the ground

τ_{res} = flame residence time or average fuel burning time

$\bar{d}_a$ = mean size of all the fuel

α_{f_o} = thermal diffusivity of dry fuel.

It is assumed that the fuel in the near vicinity of the fire front is dried by the fire (so that the dry fuel moisture content is approximately 2 percent). Note that the mean size fuel burning time could also be calculated using the procedure described in Section III-B for determining the on-ground fire-brand burning time [Eqs. (5), (6)]. However, Eq. (5) was derived from experiments in which single fuel sticks were burning. It would not apply to fuel burning in fire fronts where many heat sources are present, much higher rates of heating are encountered, and the burnout times of a stick much shorter. Equation (13) for τ_{res} is more applicable in this case. (Alternatively, Anderson [1969] indicates that there is justification for using a flame residence time which varies linearly with size.)

The convection column half-width at the interface of the high and low buoyancy zones b_o is given by

$$b_o = \frac{\dot{M}_f H_c C_r}{3.19\,\rho_\infty \left[\left(1 - \frac{T_\infty}{T_{f\ell}}\right)\frac{T_\infty}{T_{f\ell}}\,400\dot{M}_f^{2/3}\right]^{1/2} C_{p_\infty}(T_{f\ell} - T_\infty)} \qquad (14)$$

with the half-width b varying linearly from b_g to b_o, so that $b = b_g + (b_o - b_g)z/\ell$, where $z = 0$ is the ground. Equations (9) through (14) characterize the high buoyancy zone.

Muraszew [1974] utilized the Morton [1956] approach with modifications for a line source instead of a point source to characterize the low buoyancy zone. The appropriate conservation equations for mass, momentum, and energy are

$$\frac{d}{dz}(ub\,\rho_{\ell}) = \alpha' u \rho_{\infty}$$

$$\frac{d}{dz}(u^2 b\,\rho_{\ell}) = bg(\rho_{\infty} - \rho_{\ell}) \qquad (15)$$

$$\frac{d}{dz}[u b g(\rho_{\infty} - \rho_{\ell})] = 0$$

where $\alpha' = 0.274$ is the low buoyancy zone air entrainment coefficient, ρ_{ℓ} is the density, and b is the half-width. At the interface $z = \ell$, $u = u_o$, $b = b_o$, and $\rho_{\ell} = \rho_{f\ell}$. The solution for $z \geq \ell$ is

$$u = u_o$$

$$b = 0.274\,(z - \ell) + b_o \qquad (16)$$

$$\rho_{\ell} = \rho_{\infty}[1 - (1 - \rho_{f\ell}/\rho_{\infty})b_o/b]$$

Equation (16) characterizes the low buoyancy zone.

In the presence of a horizontal wind, the column is tilted. Putnam [1965] observed that the tilt angle ϕ for a wind speed W_x is given by

$$\tan\phi = W_x/u_o \qquad (17)$$

The column centerline is tilted at the angle ϕ, measured from the vertical, with the half-width b(z) unchanged.

With the convection column characterized, the trajectory of a firebrand can be determined. Firebrands whose density and size are such that their fall velocity within the column is less than the column vertical velocity can be lifted. Tarifa [1965] showed that a firebrand in flight quickly reaches the velocity of the gas in which it is moving, with an additional downward component equal to its instantaneous fall velocity W_f. Thus, within and outside of the convection column, the firebrand trajectory is given by

$$\dot{z} = - W_f + u, \quad \dot{x} = W_x \tag{18}$$

where u = 0 outside of the column. If a vertical wind component is present, then that component is added to the right-hand side of the first of Eq. (18). The wind can be a function of position.

The fall velocity is given by

$$W_f = \left[\frac{2g \rho V_f / A}{\rho_g C_D} \right]^{1/2} \tag{19}$$

where

V_f = firebrand volume

A = its drag area

C_D = its drag coefficient

ρ = its instantaneous density

g = gravitational acceleration

ρ_g = density of the gas it is flying in (e.g., $\rho_g = \rho_{f\ell}$ in the high buoyancy zone, $\rho_g = \rho_\infty$ outside of the column, etc.)

Within the column, if $\dot{x}/\dot{z}$ is greater than the slope of the column side $(db/dz + \tan\phi)$, then the firebrand can escape the column. The smaller the size of the firebrand, the smaller W_f and the smaller the value of $\dot{x}/\dot{z}$.

Particles that are too small will not leave the column and, therefore, will not be viable spot fire threats. The critical maximum size of a firebrand is that which can be just lifted, and is given by $W_f = u_o$.

In the present work, the assumption is employed that a firebrand (which can leave the column) is ignited within the column or fire front but starts burning as it leaves the convection column. As it burns, its density decreases according to Eq. (4) with t measured from the time the firebrand leaves the column. With the diameter (or thickness) of a firebrand changing little, the instantaneous fall velocity during burning is simply

$$W_f = W_{f_o} (\rho/\rho_o)^{1/2} \tag{20}$$

where W_{f_o} is the initial fall velocity in the ambient air.

For a given firebrand density, size, shape (cylindrical or plate), and initial position in the convection column, the trajectory equations are integrated enabling the total distance traveled and the firebrand impact density to be determined. If its density in flight drops to ρ_c as determined by Eq. (6), it is assumed to have burned up at that point.

The firebrand initial position in the column is taken to be a vertical height off the ground equal to the fuel bed depth and to be uniformly distributed horizontally. Trajectory calculations show that horizontal uniformly spaced initial positions within the convection column approximately result in uniformly spaced impact, or landing, positions. The maximum impact distance for a given size, density, and shaped firebrand occurs when the firebrand is at the upstream edge (relative to the wind) of the column (if it does not burn up in flight), and, of course, the minimum when it is at the downstream edge. Thus, if N_d is the total number of potential firebrands of a given size class (with a given initial density) per unit length of fire front per unit time and ℓ_{x_d} the maximum distance traveled without burning up in flight,

then the potential rate of impact of firebrands of that size per unit area is N_d/ℓ_{x_d}. Multiplying this by the firebrand generation function F_d would give the actual number that land per unit time per unit area.

The time of flight decreases and, therefore, the impact density increases for smaller travel distances. Up to that distance for which the impact density is just large enough so that the on-ground firebrand burning time is equal to $\overline{t}_{ign}$, there is a given probability of recipient fuel ignition and, hence, of a spot fire. Within that distance, or within ℓ_{x_d} if the impact density at ℓ_{x_d} is greater than the critical, the expected number of spot fires per unit time per unit area resulting from a firebrand of a given size class is $(N_d/\ell_{x_d})\, F_d P_{ig}$. At greater distances from the front, the expected number is zero. Since larger sized firebrands will have smaller ℓ_{x_d} (and smaller N_d), the expected number of spot fires per unit area decreases with increasing distance from the fire front.

All of the components required to calculate the expected number of spot fires have been discussed except the firebrand generation function. This is discussed in Subsection D.

D. FIREBRAND GENERATION FUNCTION

The firebrand generation F_d is the probable fraction of all potential firebrands actually lifted. It depends on the intensity of the lifting mechanism and on the fuel characteristics. The generation function is expected to depend on the size and density of the firebrand, on the intensity and degree of completion of burning of the fuel, and on the nature of the fuel.

The characterization of size distribution was described in Section III-B. Besides knowing the weight fraction of a given size class, the degree of attachment to larger pieces, branches, etc., is important. While a given size firebrand could by itself be a viable spot fire threat, if it is attached to a large branch or stem of a shrub, then it is not a threat unless it becomes unattached. Available size distribution data do not distinguish between single firebrand members and those which are attached to a shrub. Even if a

potential firebrand is unattached and lying on the ground, it may be near the bottom of the ground litter and thus not readily available for lifting. Whether individual or attached, it may be consumed by the fire. If the shrub height is fairly large or the area is heavily wooded with trees, then the movement of a fuel member which is otherwise free to be lifted could be impeded. Thus, F_d depends not only on the fuel size distribution but on its configuration or arrangement. Thus, for instance, the firebrand generation function for a given size firebrand would be expected to vary for the nine fuel models mentioned in Section III-B.

The potential for lifting also depends on the column uplift force. The drag force on a firebrand depends on the velocity squared and the firebrand acceleration depends on the difference between the drag force and the firebrand weight. Since the firebrand upward acceleration then varies as $(u_o/V_{cr})^2 - 1$, the firebrand generation function was taken to depend on this factor, where V_{cr} is the fall velocity in the column for a given firebrand size, shape, and density, given by Eq. (19).

The firebrand generation function was taken to have the following functional form

$$F_d = 1 - \exp\left\{-K[(u_o/V_{cr})^2 - 1]\right\} \qquad (21)$$

where K is dependent on the fuel model and is constant for a given fuel model. Values for F_d of 0.001 to 0.02 were considered reasonable values for a convection column, with K depending on fuel characteristics and varying from 0.0005 to 0.005. (In the two cases considered in Appendix C, i.e., the Romero fire case and the logging slash, values of K of 0.001 and 0.00335, respectively, were selected.) Fuel models characteristic of open areas, with large amounts of ground litter fuel, would be expected to have larger values of K and of F_d than areas characterized with dense trees, large-sized shrub material, and a small amount of loose ground litter. Laboratory and/or field data are needed to determine the adequacy of such a functional

form and to determine K. Such data would require specification of fuel characteristics and column velocities, as well as a measure of the number and size of firebrands lifted.

E. SPOT FIRE REGIMES AND HAZARD

The methodology for predicting the ignition points (spot fires) induced by firebrands generated by a steady-state convection column was presented in the preceding sections. For a firebrand-induced ignition point to become a threat, the firebrand must travel to its impact point, and ignite the recipient fuel; then the resulting ignition point must spread before the main fire front reaches the ignition spot. If the main fire front overruns the ignition location before a spot fire can begin spreading, then that ignition point does little to influence the fire behavior and is not a threat. Thus, firebrands that fall too close to the fire front do not influence its behavior.

Spot fires that are initiated sufficiently far from the main fire front can begin to spread out before the main front engulfs the ignition point. Then these spot fires produce a "tongue" of fire jutting ahead of the main front. If a number of these spot fires occur almost simultaneously and close to each other, then there is a danger of rapid coalescence of a number of spot fires into another broad fire front out ahead of the main front. When the main front catches up to the initiation location of this induced front, which itself is spreading and moving forward, the result is in effect a jump in the fire front position. These discontinuous jumps can result in a much more rapid rate of fire front progress than would a conventional fire spread.

Thus, there is a zone, or region, close to the main front where recipient fuel ignition does not change the fire behavior or increase the hazard from the fire. There is also a maximum distance (from the instantaneous front location) beyond which no spot fires induced by the steady-state convection column can occur because the firebrands that do travel farther do not land with sufficient mass to pose an ignition threat. For a given size firebrand, there is a critical impact density below which it will not ignite the recipient

fuel [from Eqs. (5) and (6), with $\rho = 1.1\rho_c$], and a specific in-flight burning time associated with that impact density [from Eq. (4)]. From a trajectory calculation, the maximum travel distance that results in an impact density at least as large as the critical density is obtained; it is called L_{max}. There is a critical size firebrand which results in the largest maximum travel distance, L_3 (L_3 = greatest L_{max} over all firebrand sizes), while still remaining an ignition source threat. Larger firebrands are not lifted as high in the convection column and fall more quickly outside of the column and, therefore, do not travel as far. Smaller firebrands either do not leave the column or, if they do, burn faster and thus have a shorter travel distance (or shorter burning time) over which they are still an ignition threat. Thus, the short-range spot fire danger zone is that region between the maximum threat distance and the distance within which the main front will overrun any ignition point.

The distance within which any spot fire will be overrun before it can spread (L_1) depends on the spread rate R of the main fire front (see Figure 3a). This distance is equal to the distance the front advances in a time equal to the flight time of a firebrand, plus the time it takes the recipient fuel to be ignited, plus the time it takes the fire to start spreading. The fire must start to spread before the ignited fuel burns out. Thus, the spread time is the on-ground burn time of the recipient fuel. Since the dead fuel is the more easily ignited, the spread time is taken to be the on-ground burning time of the average dead fuel size, as determined by Eqs. (5) and (6) with ρ_o and $\bar{d}$ (the average dead fuel size) replacing ρ_{imp} and D_{imp}. Since $\bar{d}$ will usually be less than 1.25 cm, $\rho_c/\rho_o = 0.05$. With $\rho = 1.1\rho_c$ in Eq. (5), the spread time is given by

$$\bar{t}_{spr} = 43.3\left(\frac{M}{2}\right)^{0.44} \bar{d}^2 \ell n(0.95/0.005) \qquad (22)$$

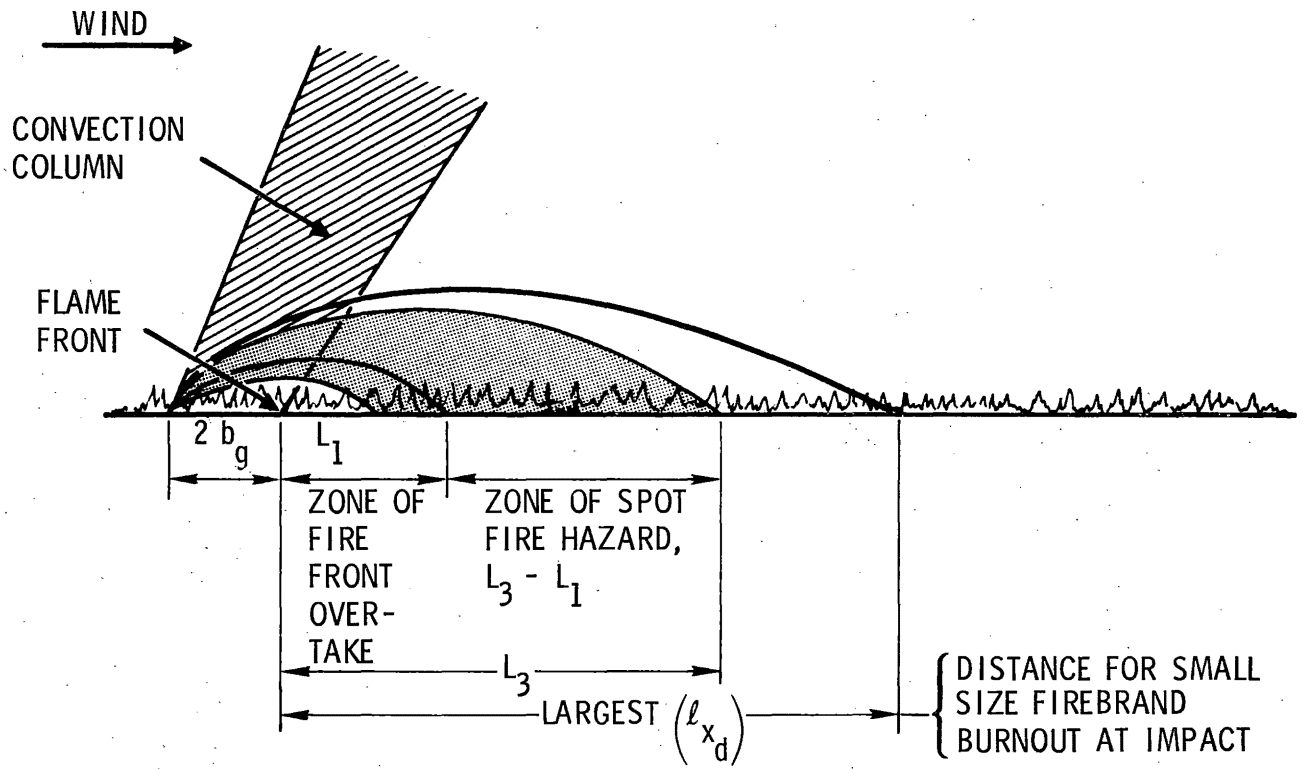

(a) Spot Fire Hazard Zone

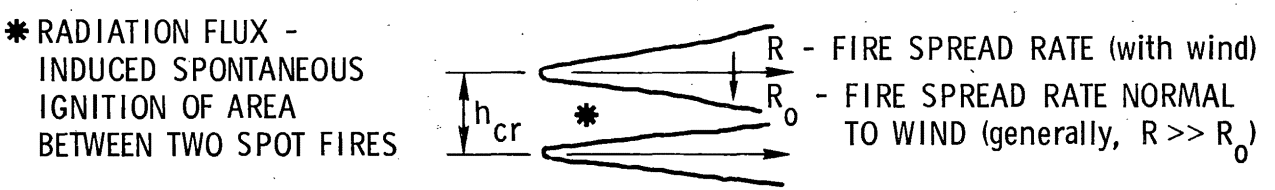

(b) Spot Fire Rapid Coalescence

Figure 3. Spot Fire Criticality

This would normally be the largest time component in determining L_1. Thus, L_1 is given by

$$L_1 = R[\bar{t}_{f\ell} + \bar{t}_{ign} + \bar{t}_{spr}] \tag{23}$$

The mean flight time to travel a distance L_1 is determined, by iteration, from trajectory calculations, and $\bar{t}_{ign}$ is given by Eq. (3).

The largest maximum travel distance (and the critical firebrand size) for which the impact density is greater than or equal to the critical impact density is determined by calculating the critical impact density for various sizes and determining from trajectory and in-flight burning calculations which size travels the farthest while still having an impact density at least as large as the critical density. The critical density for a given size is determined from Eqs. (5) and (6). If the size of the maximum threat range firebrand is less than 1.25 cm (as is usually the case), then $\rho_c/\rho_o = 0.05$ and, with $\rho = 1.1\ \rho_c$, Eq. (5) for ρ_{cr} for a given size firebrand becomes

$$\rho_{cr}/\rho_o = 0.05 + 0.005 \exp\left[\bar{t}_{ign}/43.3\left(\frac{M}{2}\right)^{0.44} D_o^2\right] \tag{24}$$

After obtaining ρ_{cr} versus D_o, the maximum threat range L_3 and the critical size are determined from trajectory calculations utilizing the convection column characterization and Eqs. (4), (18) through (20).

The region located between the distances L_1 and L_3 ahead of the instantaneous fire front (and convection column) is where spreading spot fires can begin (see Figure 3a). If a region of depth L_3 were devoid of fuel, then there would not be a short-range spot fire threat. A fuel break should be of a depth greater than L_1. A fuel break less than or equal to L_1 would have no significance in spot fire hazard reduction. The L_3 is the maximum fuel break depth needed in order to essentially eliminate the short-range spot fire threat.

The distances L_1 and L_3 depend on the fuel, wind, and terrain characteristics. All three affect the fire front spread rate R (R increases strongly with an increase in wind or uphill slope angle), which directly affects L_1. The L_3 also is affected by R since the convection column uplift velocity increases with R. The wind directly affects the firebrand travel distance. The increase in L_1 and L_3 with increasing wind and uphill slope angle is illustrated in the first example of the Romero fire in Appendix C (see Table C-5). For instance, L_3 increases more rapidly than linear with increasing wind. In general, the rate of change with wind or slope depends on the fuel properties. The effect of wind and slope on R for given fuel properties can be obtained from the Rothermel [1972] formulation. Note that L_1 and L_3 do not depend on the number of spot fires that can occur, and hence do not depend on the value of the ignition probability or the firebrand generation function. They do depend on the trajectory, in-flight burning, and on-ground burning analysis.

The probability of spot fires between L_1 and L_3 is the only one that needs to be considered. Thus, the only size firebrands which need to be considered are those that fall between L_1 and L_3 with an impact density at least as large as the critical density. The largest size that needs to be considered is that which has a maximum travel distance (when initially located at the extreme upwind edge of the convection column) equal to L_1. The smallest size is that which leaves the convection column and falls within L_1 and L_3 with $\rho_{imp} \geq \rho_{cr}$.

To calculate the expected number of spot fires, subdivide the size interval of firebrands between the largest and smallest sizes to be considered. The expected rate at which firebrands are lifted, per unit length of fire front, within a size subdivision is $F_d N_d$, where N_d is given by Eq. (1). The characteristic size to be used in the trajectory and burning calculations is taken to be d_1 (the diameter at the low end of the interval). The maximum impact travel distance ℓ_{x_d} is calculated for that size, and the expected rate at which

firebrands of that size subinterval land in a unit area is $F_d N_d / \ell_{x_d}$. (As discussed in Section III-C, the distribution of firebrands landing is approximately uniform between the front and ℓ_{x_d}. If ℓ_{x_d} is larger than L_{max}, the impact density is less than the critical density for landing distances larger than at least L_3, and the firebrands that land at those distances are not a threat.) Within the maximum threat distance for a given size firebrand, the expected or most probable number of ignition points per unit time per unit area is $F_d N_d P_{ig} / \ell_{x_d}$. The total expected rate in a given area is obtained by summing up the total over all the size subintervals of firebrands which are threats in that area and multiplying by the area; to get the total number of ignition points in a given area in a given time interval, further multiply by the time interval.

The foregoing formulation gives the mean number of spot fires occurring in a given area in a given time. To obtain the probability that a specified number will occur, the probability distribution function for spot fire occurrence must be known. Given that the occurrence of a spot fire is a discrete random event with the mean number of occurrences in a given area $\Delta A(x)$ within a time Δt given by

$$\lambda = \sum_d F_d N_d P_{ig} (\Delta A)(\Delta t) / \ell_{x_d} \tag{25}$$

then the probability of having n spot fires within ΔA, Δt is given by a Poisson distribution with

$$P(n) = \frac{\lambda^n \exp(-\lambda)}{n!} \tag{26}$$

Then, for instance, the probability of having at least one spot fire within ΔA, Δt is $P(\geq 1) = 1 - P(0) = 1 - \exp(-\lambda)$. The area $\Delta A(x)$ is always located a distance x from the instantaneous fire front location, and thus moves forward with the front.

Appendix C-I, II gives examples for two forest fire conditions. One is for the Romero fire which represented a light dead fuel loading with a relatively small fire spread rate. The other is for a logging slash case with a large dead fuel loading (lb/ft^2), a smaller average fuel size, higher spread rate and, consequently, a more intense convection column (see Appendix C for details). With the smaller fuel size, $\bar{t}_{ign}$ and $\bar{t}_{spr}$ are smaller than for the Romero case, and, even though the fire front spread rate R is greater, L_1 is less (44 ft compared to 66 ft). As expected, L_3 is much larger for the logging slash case (about 450 ft compared to 92 ft for the Romero case) so that the danger zone L_3-L_1 is much larger (by a factor of more than 15). The total expected mean rate of spot fire initiation is also much greater for the logging slash case, being 2460 compared to 49 per min per 100 ft of front for the Romero case. For either case, the probability of having at least one spot fire in the danger zone per minute per 100 ft of front is near unity.

Figure 4 shows the maximum impact distance ℓ_{x_d} for the two cases at the same wind velocity of 12 mph. The effect of the more powerful convection column of the logging slash fire is evident in the larger size and distance of the firebrand generated.

The effect of wind on the spot fire danger distance L_3 and, hence, on the fuel break depth, can be assessed from Figure 5. The distance L_3 increases with the wind velocity.

Given the expected mean rate of spot fire occurrence and the probability distribution function, the probability that coalescence of several spot fires occurs can be estimated. Rapid flame coalescence some distance ahead of the fire front could occur if two or more spot fires are started close enough so that the combined radiation flux from the spot fire flames will bring the fuel in the middle to the ignition point. We should consider that the ignition is of the spontaneous ignition type (see Figure 3b).

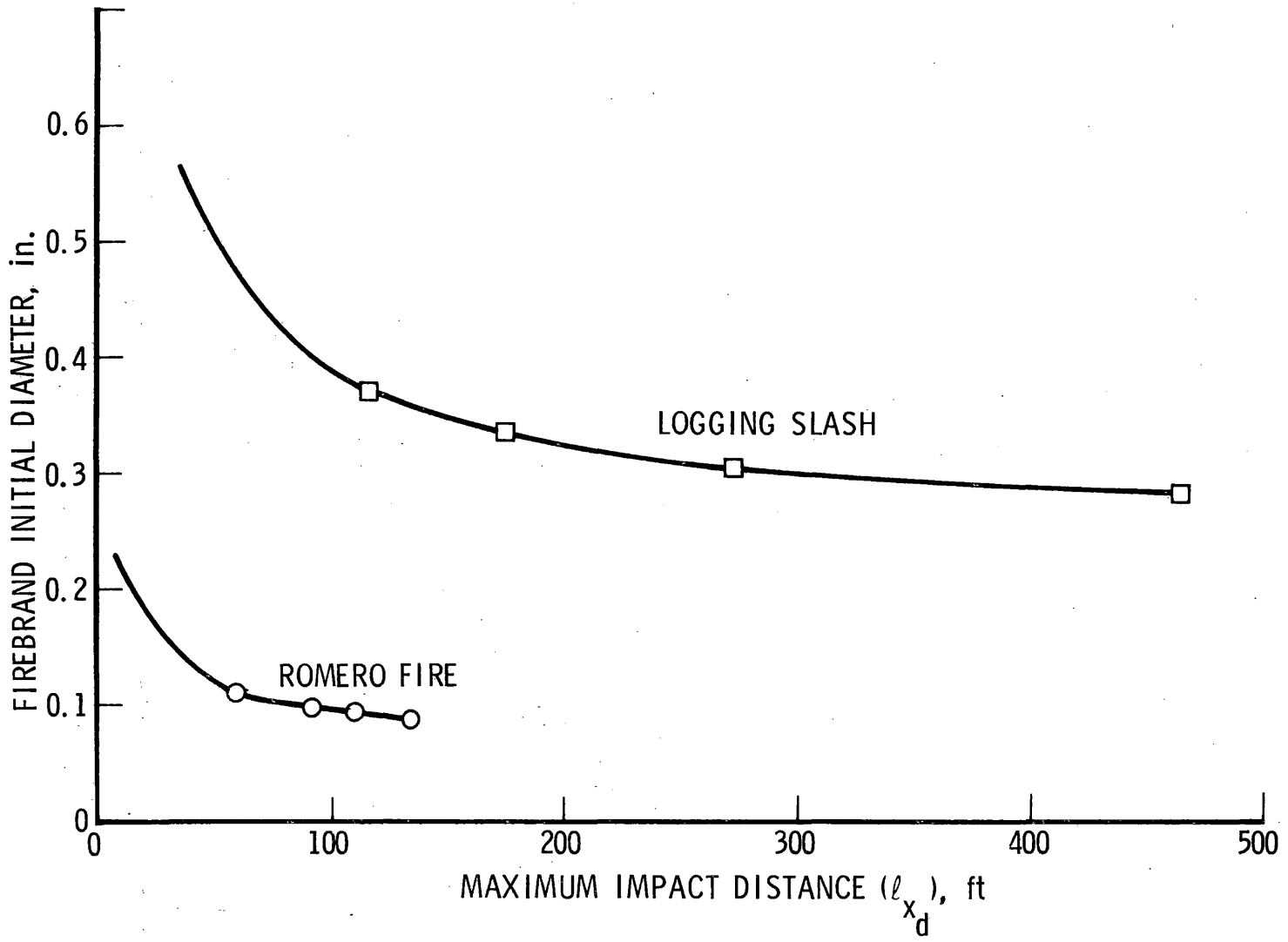

Figure 4. Maximum Firebrand Impact Distance as a Function of Initial Diameter (12 mph wind)

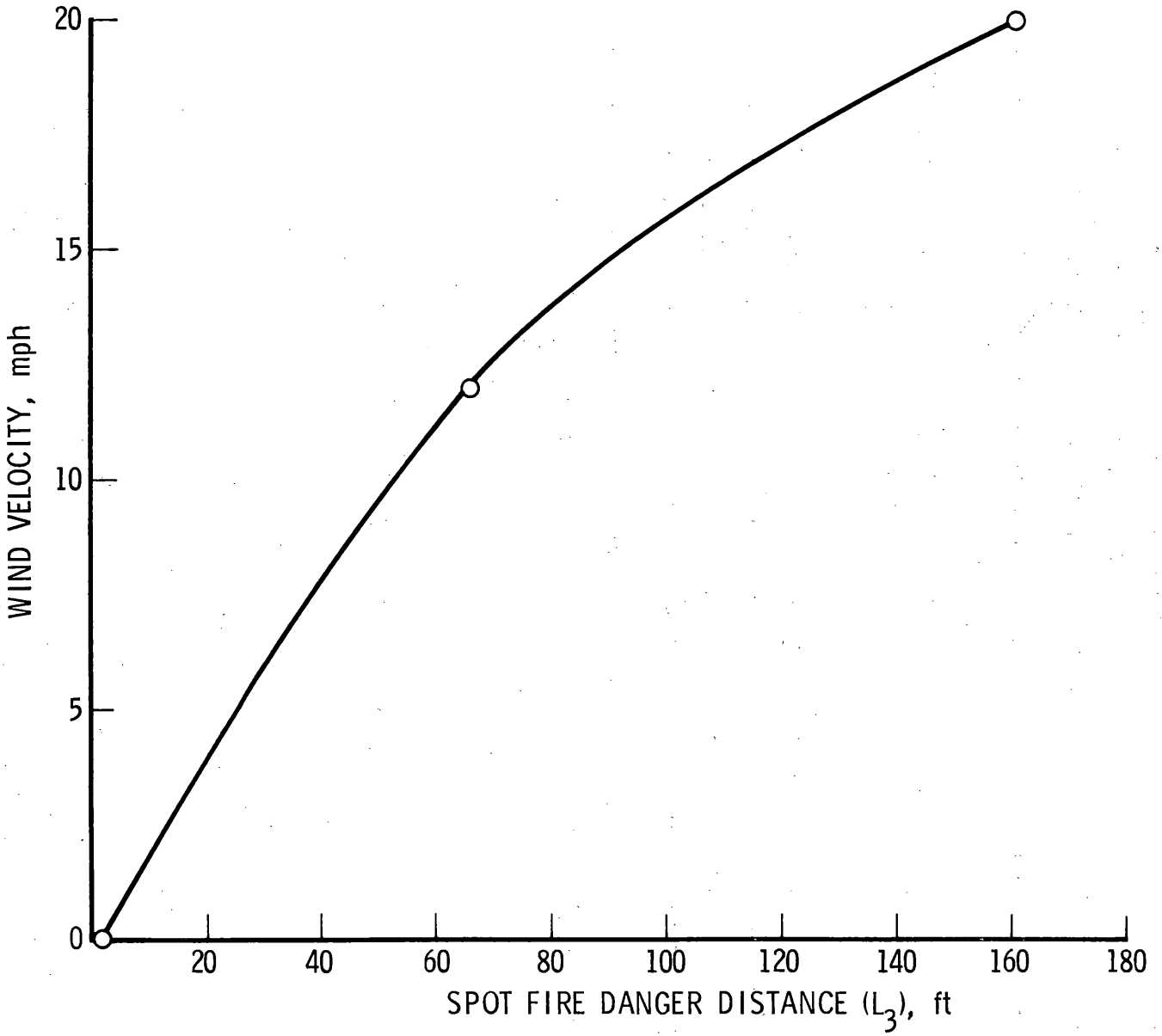

Figure 5. Effect of Wind Velocity on Spot Fire Hazard Distance, L_3

The problem of virgin fuel ignition by firebrands was already discussed in Section III-B. Of interest here is the heat flux required for fuel ignition. In this respect, the work of Simms [1960 and 1963], Simms and Law [1967], Martin [1964], and Stockstad [1975] may be quoted, although very little of that work, except for Stockstad's experiments, was applicable to natural fuels.

Stockstad was heating cheatgrass by radiation and observed that the total effective heat flux to produce spontaneous ignition was 5.8 cal/cm^2 with fuel moisture content up to 18 percent and approximately 10 sec ignition lag, which corresponded to an approximate average effective heating rate of 0.6 cal/cm^2-sec.

On the other hand, Simms and Law [1967], using fiber and wood boards of thickness from 1.9 to 2.5 cm, required a total heat flux of at least 25 cal/cm^2. Increase in moisture content from 0 to 20 percent increased the minimum required rate of heating by approximately 10 percent.

We shall consider that the heat flux required is between the two values quoted, and a value of Q_i = 14 cal/cm^2 is assumed.

The average radiation flux from a spot fire flame can be calculated from

$$\overline{q}_r = \epsilon \cdot \eta \ \delta \cdot T_{f\ell}^4 - \epsilon_s \cdot \delta T_s^4 \qquad (27)$$

where

η = fuel element surface absorptivity assumed 0.6 (Muraszew [1974])

ϵ = flame emissivity, assumed 0.23

ϵ_s = fuel element surface emissivity assumed equal to η

δ = Stefan-Boltzmann constant = $1.36 \cdot 10^{-12}$ cal/cm^2-sec-$^oK^4$

$T_{f\ell}$ = flame temperature, assumed 1100^{o}K

$\overline{T}_s$ = average recipient fuel surface temperature, assumed 400^{o}K.

Substituting the appropriate values in Eq. (1), $\bar{q}_r = 0.25$ cal/cm^2-sec, or from two spot fire flames $\bar{q}_{rt} = 0.5$ cal/cm^2-sec. This is the heat flux emitted. The flux received at a point on the ground equals the emitted flux multiplied by the view factor at that point.

This emitted radiation flux is assumed to continue during the residence time (or burnout time) of the average size of all fuels (i.e., mean of the dead and live fuel) with some average moisture content. This residence time t_{resid} can be calculated from Eqs. (5) through (7).

The average required heating rate is $\bar{q}_i = Q_i / t_{resid}$. If it is assumed that there will be wind-caused heat losses from the fuel surface equal to 40 percent of q_i, then the ratio of $1.4\ q_i / 2q_r$ will define the limiting required view factor for the flame; thus it may be assumed that the height of the flame is equal to the fuel bed height and that the flame is inclined outward 30 deg from the vertical, and a critical distance (h_{cr}) for spontaneous ignition of the median strip between two spot fires can be determined (using, for instance, the Keith [1962] planar source view factor graphs).

For large fuel bed heights (and reasonable burning time), values of h_{cr} of a few feet are obtained. Since the ground very near a spot fire will be susceptible to radiation-induced ignition, the added flux from another fire a distance h_{cr} away is sufficient to ignite the fuel midway between them (at a distance of $h_{cr}/2$ from either one), so that small values of h_{cr} are reasonable. However, for small values of fuel bed height and/or t_{resid}, the values of h_{cr} given by this method may be too small to be of practical use (less than 1 ft, say). When this is the case, rapid coalescence will be more likely to occur due to the natural spread and merging of two adjacent spot fires. Then h_{cr} is determined as follows: In a time t_{resid}, two adjacent fires will each spread a distance $R_o t_{resid}$ in the direction normal to the wind (parallel to the main fire front), so that $h_{cr} = 2\ R_o t_{resid}$ for this case. Figure 3b illustrates coalescence.

Rapid coalescence of two spot fires will occur if they are initiated within a distance of h_{cr} and a time of t_{resid} of each other. Generally, h_{cr} will be on the order of a few feet ($h_{cr} \sim 2$ ft for the two examples in Appendix C-I, II). The former is a radiation-induced case while the latter is a natural merging case. For coalescence to create a secondary fire front of sufficient width to be of concern, coalescence of several spot fires is needed. Take the number of spot fires needed to coalesce to be at least Y and the area ΔA over which they must be initiated to be (1) Yh_{cr}. Then the mean number of spot fires occurring within one such area within a time t equal to t_{resid} is λ, as given by Eq. (25). Hence, the probability of coalescence occurring within an area Yh_{cr} within a time t_{resid} is

$$P[\geq Y, \lambda(Yh_{cr}, t_{resid})] = 1 - \sum_{n=0}^{Y-1} P[n, \lambda]$$

$$= 1 - \exp(-\lambda) \sum_{n=0}^{Y-1} \frac{\lambda^n}{n!} \qquad (28)$$

The probability that coalescence will occur anywhere within an area A and time t is given by

$$P[\geq Y; A, t] = 1 - \left[\exp(-\lambda) \sum_{n=0}^{Y-1} \frac{\lambda^n}{n!} \right]^{(A/Yh_{cr})(t/t_{resid})} \qquad (29)$$

since the term which is subtracted from 1 in Eq. (29) is the probability that coalescence does not occur within t/t_{resid} critical time periods in any of the A/Yh_{cr} number of areas of size Yh_{cr}.

The greater the rate of spot fires occurring in an area, the greater the probability of coalescence. In the two examples in Appendix C, the probability, for instance, that at least four spot fires will coalesce anywhere in the respective danger zones in 100 ft of fire front width within an hour is 23 percent for the Romero case and 99.97 percent for the logging slash case. Figure 6 illustrates the probability of coalescence of four spot fires for the Romero fire and for the logging slash fire subzone six, which is similar in size and location to the entire Romero fire zone L_3-L_1. The abundance of loose, dead wood sticks available with the logging slash is reflected in much greater spot fire and spot fire coalescence hazard. For the number of spot fires for the two cases, compare Tables C-2 and C-8, and for coalescence probability, Tables C-2 and C-9.

Appendix C-I, II gives more details of calculations based on the methodology outlined above. Data on fuel size distribution, trajectory, in flight and on-ground burning, fuel break, mean number of spot fires, and coalescence results are presented. The flow diagram given in Appendix A illustrates the methodology.

The major uncertainty in the calculations is in the firebrand generation function. The number of spot fires due to a given size class is directly proportional to F_d, as shown in Eq. (25). For small enough values of K (such as for the range given in Section III-D, or the values used in the examples in Appendix C), F_d is directly proportional to K. The probability of coalescence is very strongly dependent on F_d (or K). For example (see Table C-4), for Y = 4, and h_{cr} = 2 ft for the Romero case, the probability of coalescence occurring within one hour in a 100-ft length of front was 23.3 percent for the nominal K used (0.001) and 97.8 percent and 1.4 percent for K a factor of two bigger and smaller, respectively. The great sensitivity of the probability of coalescence to the value of the parameter K emphasizes the need for some field observations of spot fires and of the spot fire coalescence.

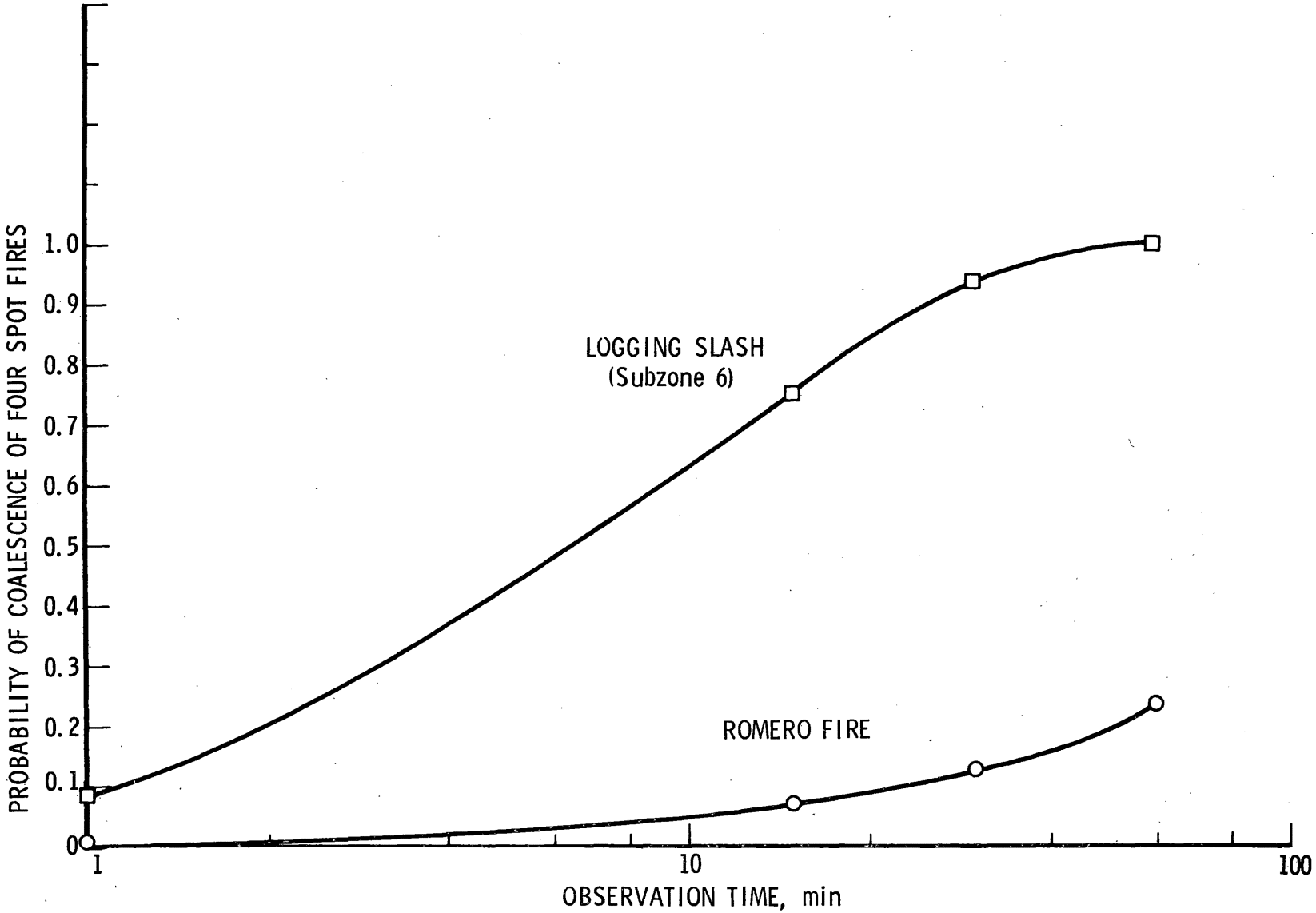

Figure 6. Probability of Spot Fire Coalescence

The sensitivity of probability of coalescence to h_{cr} (or t_{resid}) is shown in Table C-3. As expected, recipient fuels easier to ignite and generating more heat (greater value of h_{cr}) have much greater probability of flame coalescence.

IV. LONG-RANGE SPOT FIRES

A. APPROACH

The basic approach taken to evaluate the long-range spot fire hazard, assuming that the lofting mechanism is a fire whirl, is similar to that described for short-range firebrands, with a few exceptions as noted below. The analytical steps will consist of the following:

a. Characterization of a fire whirl

b. Trajectories of firebrands and their condition at impact

c. Calculation of a potential number of firebrands of various sizes which could be lifted during the duration of the fire whirl

d. Assumption of a firebrand generation function

e. Calculation of the number of firebrands impacting at various distances from the fire whirl

f. Assessment of the probability of ignition of recipient fuel by falling firebrands

g. Calculation of the probable number of firebrand-caused ignition points

h. Calculation of the probability of spot fire occurrence at various distances from the fire whirl.

A brief description of these analytical steps will be given and will be followed in the latter section of this report by more detailed discussion of the key steps. A flow diagram of these steps is given in Appendix B.

The fire whirl mathematical model was generated before by the authors and presented in an earlier report (Muraszew, Fedele, Kuby [1976]). It is reviewed here in Section IV-C. Similarly, firebrand trajectories were dealt with in the earlier work of the authors. Because of large forces and accelerations associated with a fire whirl, the firebrand trajectories in and near the fire whirl are calculated using the full equations of motion. Away from the whirl, the approach used for the convection column threat is employed.

Larger firebrands and larger flight times are appropriate and their diameter, as well as density, change during in-flight burning. The trajectory analysis is also reviewed in Section IV-C.

The potential number of firebrands will be calculated, as for the case of short-range firebrands, from known loading and size distribution of dead fuels. The only difference between the approach to the short-range firebrands generated by a steady-state, continually progressing fire front and long-range firebrands generated by fire whirls is that the latter is a short-lived but intense phenomenon of an average duration of a few minutes or less which will limit the total number of firebrands that could be lifted.

The firebrand generation function will be similar to that adopted for short-range firebrands, but the much higher uplift velocities of a fire whirl will result in a greater fraction of firebrands lifted and in greater maximum size of "liftable" firebrands.

From the firebrand generation function, the probable number of firebrands lifted of various size classes up to a maximum that can be lifted as well as their impact distance and the remaining mass at impact can be calculated. In this case, the impact distance may vary from zero to several miles, depending on the fire whirl and firebrand characteristics, initial firebrand location in the fire whirl, and the ambient wind.

When considering the probability of ignition of the recipient fuels by firebrands, the combustion state of long-range firebrands, with flight times of 100 sec or more, must be taken into account. Experiments carried out earlier (Muraszew, Fedele, Kuby [1976]) indicate that such long-range firebrands upon impact will be predominantly in glowing combustion and that sufficient firebrand mass must remain after impact to bring an average element of dead fuel to its ignition temperature. Applying the National Fire-Danger Rating System ignition component [see Eq. (8)] to those firebrands that are able to ignite the recipient fuel, results in the probability of ignition and a probable number of ignition points. For firebrands that fall at short ranges, the ignition probability approach is the same as that described in Section III-B.

The assessment of the probability of spot fires at various distances over the period of fire whirl duration is based on the same distribution law as that discussed in Section III-E. Because of the limited fire whirl diameter and short lifetime, the short-range hazard from a fire whirl is usually small compared to that of a convection column. The number of short-range spot fires initiated in a given area by a fire whirl is usually less than that of a convection column, so that a rapid flame coalescence due to a fire whirl is generally not a hazard.

B. FUEL CHARACTERISTICS AND FUEL IGNITION

Fuel characteristics pertinent to formation of firebrands were discussed in Section III-B and need not be repeated here. Calculations leading to the definition of a firebrand mass at impact are similar to those described in Section III-B, although the trajectory model from which the firebrand in-flight burning time is computed is different within and near the fire whirl and is described in Section IV-C.

The ignition mechanism of the recipient fuel by firebrands falling close to the fire whirl will be the same as that for short-range firebrands discussed in Section III-B, but for the long-range firebrands this mechanism will be different.

In the course of the NFFL experimental work on in-wind burning of wood sticks and plates, it was observed that after 30 sec or less following ignition the initial flaming combustion was replaced by a glowing combustion that continued to the end of burning (Muraszew, Fedele, Kuby [1976]). It was also observed that, in some cases, a glowing firebrand burst into flame for a few seconds after being removed from the wind (simulating impact), returning thereafter to glowing combustion. However, this phenomenon occurred only sporadically and was of such a short duration that the condition of glowing (rather than flaming) combustion was predominant and was assumed here as typical for the impact condition of long-range firebrands, which typically have flight times of 100 sec or more.

To establish the go-no-go ignition-ability criteria for glowing firebrands, we shall consider the case of a glowing firebrand falling on an element of dead fuel and heating it, with the firebrand surface temperature remaining constant, until the temperature on the back face of the fuel element reaches the pyrolysis temperature of the hemicellulose--the most reactive constituent of wood.

If we assume the glowing firebrand surface temperature to be 580°C (Muraszew [1974]) and the heated fuel element back surface to be 230°C (hemicellulose decomposition temperature is 200°C to 260°C), then, for a case of a flat plate heated by a constant temperature, the Fourier number can be determined from the P. J. Schneider [1963] temperature response charts for the temperature parameter 230-30/580-30 = 0.364, where 30°C is ambient temperature of the recipient fuel. The Fourier number F_o for this temperature parameter is 0.28, and the ignition time

$$\bar{t}_{ign,g} = 0.28 \frac{\bar{d}^2}{\alpha_f} \tag{30}$$

where $\bar{d}$ is mean dead fuel thickness, cm, and α_f is fuel thermal diffusivity, cm^2/sec.

To consider the fuel moisture effect, α_f can be expressed as a function of that moisture. Since $\alpha_f = k_f/c_f \cdot \rho_f$ where k_f, c_f and ρ_f are fuel thermal conductivity, specific heat and density at a given moisture level, expressing these parameters as a function of fuel moisture will give the required dependence of α_f on fuel moisture. Simms and Law [1967] quote such relationships for the three fuel parameters. Using these relationships and calculating α_f for various moisture contents, the following approximate equation is derived:

$$\alpha_f = \alpha_{f_o} 10^{-0.0151 \frac{M}{M_{ref}}} \tag{31}$$

where

α_{f_o} = thermal diffusivity at 0 moisture (typical $1.74 \cdot 10^{-3}$ cm^2/sec)

M_{ref} = reference moisture of 2 percent

M = fuel moisture, percent (≤ 20 percent)

For the case of very fine fuels, the combustion state of the firebrand (whether glowing or flaming) has little influence on the ignition time of the fuel in contact with the firebrand, and $\overline{t}_{ign}$ as given by Eq. (3) is appropriate. Thus, Eq. (30) is used for flaming firebrands unless $\overline{d}$ is small enough so that $\overline{t}_{ign,g}$ is less than $\overline{t}_{ign}$, for which case the latter is then used for the ignition time.

The ignition time calculated from Eq. (30) [or from Eq. (3) if $\overline{t}_{ign,g} < \overline{t}_{ign}$] is compared against the firebrand on-ground burning time (residence time) t_{res} calculated from Eq. (5), and, for the ignition to occur, it is necessary that

$$\overline{t}_{ign,g} \leq t_{res} \tag{32}$$

From that ignition criterion, firebrands with insufficient energy potential left after impact are discounted as ignition hazards, and, for those which constitute a hazard, ignition probability is calculated based on the previously quoted National Fire-Danger Rating System data with the packing ratio correction.

C. FIRE WHIRL AND FIREBRAND TRAJECTORY

From earlier work (e.g., Muraszew [1974]), it appeared that a normal thermal convection column formed above a fire front is not capable of producing long-range firebrands. Historical data and observations show that fire whirls may be sufficiently intense to lift fuel members to considerable heights and produce long-range spot fires. Fire whirls are tornado-like

regions of hot, swirling gas which can be generated by intense fires. Muraszew, Fedele, and Kuby [1976] performed subscale fire whirl experiments and developed a model for the prediction of sub- and full-scale fire whirl fluid mechanical properties and for the trajectory of a firebrand generated by a fire whirl. The model is reviewed briefly here.

The fire whirl geometry and nomenclature are shown in Figure 7. The strength Γ and vertical extent z_e of the initiating external circulation and the properties of the fuel are taken to be known inputs. The specific fuel properties required are the mean fuel size $\bar{d}_a$ and the fuel mass burn rate per unit area in the absence of wind, swirl, or slope ($\rho_b R_o$, lb_m/ft^2-sec). The latter can be obtained from the Rothermel [1972] formulation. The values of Γ and z_e depend on the wind, terrain, and the fuel. The prediction of fire whirl initiation and the associated Γ and z_e is one of the remaining tasks requiring completion.

The analysis couples the fire whirl core with the ground boundary layer inflow which feeds the core and with the burning fuel. Equations for radially averaged core variables are obtained by radial integration of the core mass, radial momentum, and axial momentum equations from the core centerline to the core-ambient air interface, utilizing the Byram and Martin [1970] formulation for the shape of this interface. An overall mass balance equation between the boundary layer inflow, the fuel mass addition, and the core flow, and an equation for the convective heat transfer at the core-burning fuel surface provides the coupling and closes the set.

The resulting equations applicable for a full scale fire whirl are

$$a/a_o = (1 - z/z_e)^{-1/2} \tag{33}$$

$$u/u_o = 1 - z/z_e \tag{34}$$

$$T(^oR) = 15{,}120\, z_e^{-0.2255} \Gamma^{0.0745} (\rho_b R_o)^{0.378} \tag{35}$$

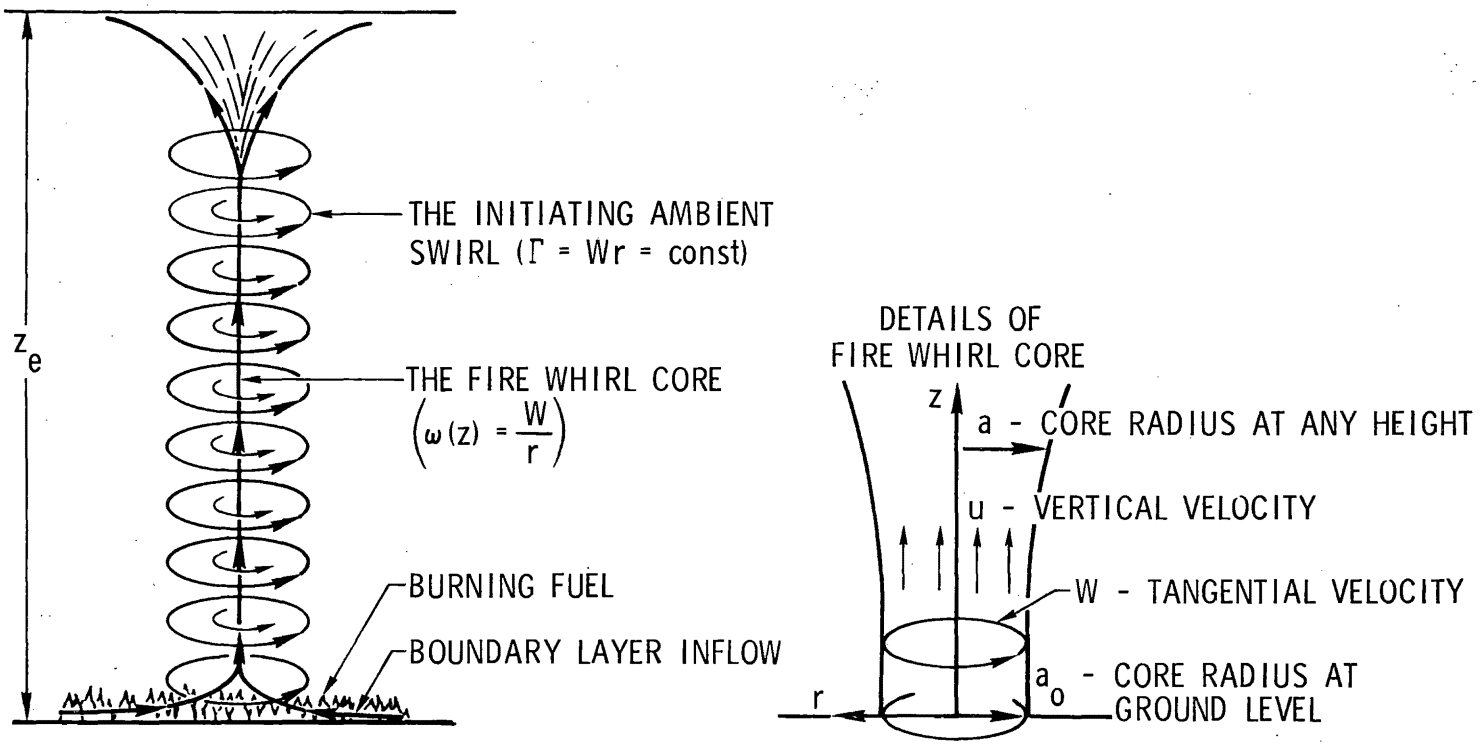

Figure 7. Fire Whirl Geometry

$$\rho_w = \rho_\infty T_\infty / T \tag{36}$$

$$(\rho_\infty - \rho_w)\, g a_o^2 = \rho_\infty \Gamma^2 / 2 z_e \tag{37}$$

$$\pi \rho_w u_o a_o^2 (C_p T - C_{p_\infty} T_\infty) = \dot{M}_f Q_c \tag{38}$$

$$\rho_b R'/\rho_b R_o = 1 + \frac{\alpha P_r^{*-2/3} C_{p_\infty} T_\infty \rho_\infty \sqrt{\frac{v_\infty \Gamma}{2 a_o \bar{d}_a}}}{\rho_b R_o Q_i} \left[\left(\frac{T}{T_\infty}\right)^{1.14} - \left(\frac{T_s}{T_\infty}\right)^{1.14}\right] \cdot$$

$$\cdot \left(0.5 \frac{\rho_w}{\rho_\infty} + 0.5 \frac{\rho_s}{\rho_\infty}\right)\left[\left(\frac{T}{T_\infty}\right)^{0.6} \frac{\rho_\infty}{\rho_w} + \left(\frac{T_s}{T}\right)^{0.6} \frac{\rho_\infty}{\rho_s}\right]^{1/2} \tag{39}$$

$$\dot{M}_f = \rho_b R' \pi a_o^2 \tag{40}$$

where

$$\alpha = 0.00513 \Gamma^{0.313} (\rho_b R_o)^{-1.085}$$

and

$\rho_b R'$ = fuel mass burn rate per unit area in the presence of a fire whirl

$\dot{M}_f$ = core fuel burn rate (with swirl), lb_m/sec

u_o, u = core velocity at the bottom of the core and at any height z.

For brevity, the other quantities are not defined here but are in the nomenclature section.

Equations (35) and (36) determine T and ρ_w, and Eqs. (37) through (40) are simultaneously solved for a_o, u_o, $\rho_b R'$, and $\dot{M}_f$. Equations (33) and (34) then determine u(z) and a(z).

Given the core fluid mechanical properties, the next step is to determine the trajectory of a firebrand within the fire whirl core, in the region just outside the core where the external swirl, or circulation, is dominant, and then in the region beyond the swirl where the prevailing wind is the driving force. The core-ambient air interface given by Eq. (33) is the boundary between the core and the external swirl regions. The boundary between the swirl and ambient wind regions is taken to be that radius where the swirl velocity equals the wind velocity, with a maximum position of 10 a_o. The wind is allowed to have a vertical and a horizontal component and to vary with x and z, where x is the direction of the horizontal wind component.

The time a firebrand spends in the core and external swirl regions is small compared to its total flight time. Therefore, firebrand burning is considered to take place in the wind region, with ignition occurring earlier.

The wind tunnel and drop test experiments of Tarifa [1967] indicate that the flight of a firebrand can be predicted by assuming that the firebrand flies in its maximum drag orientation with constant drag coefficient. The equations of motion of a firebrand in the core region are

$$m\ddot{z} = \frac{1}{2}\rho_w C_D A[(u-\dot{z})^2 + \dot{r}^2 + (W-r\dot{\theta})^2]^{1/2}(u-\dot{z}) - mg \tag{41}$$

$$m(\ddot{r}-r\dot{\theta}^2) = \frac{1}{2}\rho_w C_D A[(u-\dot{z})^2 + \dot{r}^2 + (W-r\dot{\theta})^2]^{1/2}(-\dot{r}) \tag{42}$$

$$m(r\ddot{\theta}+2\dot{r}\dot{\theta}) = \frac{1}{2}\rho_w C_D A[(u-\dot{z})^2 + \dot{r}^2 + (W-r\dot{\theta})^2]^{1/2}(W-r\dot{\theta}) \tag{43}$$

where r, θ, z are the firebrand coordinates, ρ_w is the mean fire whirl density, and u, W are the fire whirl vertical and azimuthal velocities, with $W = \Gamma r/a^2$. Initially, the firebrand is at rest at z = 0 at some arbitrary values of r, θ.

Within the core, the firebrand is lifted and also centrifuged outward until it leaves the core. The closer it is initially to the fire whirl centerline, the higher in the core it will be lifted before it leaves the core and goes into the external swirl region. In the swirl region, the trajectory equations are the same except that ρ_w is replaced by ρ_∞, u = 0, and the azimuthal (swirl) velocity is given by $W = \Gamma/r$.

The firebrand continues to be centrifuged outward until it enters the ambient wind region, where it burns and is carried by the ambient wind. In this region, the accelerations are not as great as in the core or swirl regions, and Tarifa's [1965] observation that the firebrand quickly attains the velocity of the wind with an additional downward velocity component of W_f can be used. Thus, the full equations of motion are used upon initial entry into the wind region, and, when the firebrand has slowed down so that it is essentially moving with the wind, the equations

$$\dot{z} = W_z - W_f \tag{44}$$

$$\dot{x} = W_x \tag{45}$$

are used, where W_z and W_x are the vertical and horizontal wind components.

These equations are integrated until the firebrand hits the ground or burns out in flight. For flight times and firebrand sizes of interest here, the diameter, as well as the density, changes during in-flight burning. Burnout in flight is assumed to occur when the firebrand density or diameter reaches 5 percent of its original value. The density change of the burning firebrand is given by Eqs. (4) and (7), with t replaced by $t - t_3$, where t_3 is the time of entrance into the wind region. Since the firebrand diameter changes, the instantaneous fall velocity for a cylindrical firebrand is not given by Eq. (20). [For a plate-like firebrand, the thickness still changes little and Eq. (20) applies.] However, Tarifa [1967] found that W_f/W_{f_o} is a unique function of a parameter B:

$$B = 2.6 \frac{W_{f_o}}{D_o} \left(\frac{W_{f_o} L_o}{\upsilon_\infty} \right)^{-0.4} \left(\frac{\rho_\infty}{\rho_o} \right)^{1.3} (t-t_3) \tag{46}$$

Tarifa's experimental results of W_f/W_{f_o} versus B were fitted into a two-piece analytical form

$$\begin{aligned} W_f/W_{f_o} &= 1 - 2.5B^2 && \text{for } W_f/W_{f_o} \geq 0.9 \\ W_f/W_{f_o} &= (10/9)(1 - 0.2B)^{2.5} && \text{for } W_f/W_{f_o} < 0.9 \end{aligned} \tag{47}$$

The diameter change of a burning cylindrical firebrand can then be obtained from

$$D/D_o = \frac{(W_f/W_o)^2}{\rho/\rho_o} \tag{48}$$

with ρ/ρ_o determined from Eq. (4).

Using the above formulation, the impact density, size, and travel distance for a given firebrand lifted from some initial position within a fire whirl can be determined. The initial azimuthal location $\theta(0)$ can make about a ±200-ft difference (depending on the wind and fire whirl characteristics) in the firebrand travel distance, depending on whether the firebrand enters the wind region heading against the wind or with the wind.

As enumerated by Muraszew, Fedele, and Kuby [1976], the firebrand travel distance is a strong function of its initial radial position in the fire whirl. The closer to the center, the higher it will be lifted before it is centrifuged out of the fire whirl and, therefore, the longer it will be carried by the wind before it impacts the ground. An example of a plausible fire

whirl that could be initiated for the logging slash fuel case is given in Appendix C. For that case, and for typical fire whirls, the firebrand mean travel distance, in feet (averaged over all initial θ), versus initial radial position, can be approximated by

$$\bar{x} = - \frac{(\bar{x}_{max} - 500)}{9} + \frac{(\bar{x}_{max}/90 - 5/9)}{\gamma} \qquad (49)$$

where $\gamma = r_{(t=0)}/a_o$, and $\bar{x}_{max}$ is the maximum mean travel distance for a firebrand of a particular size, shape, and density, which does not burn out in flight. Equation (49) is valid for $0.01 \leq \gamma \leq 0.1$, with $\bar{x} = \bar{x}_{max}$ for $\gamma \leq 0.01$. For $\gamma > 0.1$, the centrifuging effect severely limits the height attained in the fire whirl, so that approximately $\bar{x}(\gamma > 0.1) < 50$ ft. The firebrand generally will fall approximately within a circle having a radius of about 200 ft whose center is a distance $\bar{x}$ from the fire whirl (with x measured in the direction of the wind), the actual impact point depending on the initial value of θ. The fuel is taken to be uniformly distributed on the ground, so that any initial θ is equally probable.

The value of $\bar{x}_{max}$ for a given firebrand can be approximated in the following manner, based on full fire whirl calculations: The maximum height a firebrand will reach in the fire whirl is approximately that height where the core gas velocity is 0.61 of the firebrand's fall velocity in the core V_{cr}. (The firebrand's momentum carries it past that point where $u = V_{cr}$.) The value of z where $u = 0.61\ V_{cr}$ can be determined from Eq. (31). The wind region trajectory and in-flight burning equations are then used, with this value of z as the initial starting height, to determine $\bar{x}_{max}$. If the firebrand burns out while in flight, then $\bar{x}_{max}$ is the distance traveled up to burnout.

A firebrand which lands and burns on the ground for a time at least as long as $\bar{t}_{ign,g}$ is a threat to start a spot fire. With the firebrand impact density and diameter determined from the trajectory and in-flight burning calculation, the on-ground burning time (t_{res}) can be determined from Eqs. (5) through (7).

As for the convection column, there is a critical size firebrand which can travel the farthest while remaining a spot fire threat. Larger ones will not be carried as far and smaller ones will burn out in flight unless they travel for a shorter period of time before landing, resulting in a smaller travel distance.

The largest size of firebrand possible is that which can just be lifted. In practice, the largest size that needs to be considered is that for which $\bar{x}_{max}$ is on the order of the threat distance for the short-range firebrands from convection columns. In some cases, the maximum size is limited by the fuel sizes available. The smallest size is that which burns out in flight before it can travel farther than the threat distance from the convection column associated with the fuel burning. In practice, due to the intensity of a fire whirl, it can be assumed that any firebrand which is less than 1 in. in length or 0.5 cm in diameter will be ignited and burned up, at least partially, within the fire whirl. For a fire whirl with properties considered plausible for the logging slash case considered in Appendix C, the fuel sizes available determine the maximum size firebrand threat, and the in-whirl burnout size determines the smallest size firebrand threat. Figure 8, based on Table C-10 in Appendix C shows the $\bar{x}_{max}$ distance for cylindrical and flat plate firebrands. Note the critical size resulting in the longest distance.

The number of spot fires depends on the fire whirl lifetime. Whereas a convection column is taken to coexist with the fire front, the lifetime t_L of a fire whirl is generally on the order of only a few minutes. The movement of a fire whirl within the fire area is usually erratic, with the whirl often changing directions and repassing over the same ground. On the average, the fire whirl is assumed to travel forward with the fire front at the front spread rate R. The area swept out by the fire whirl in a time t_L is approximately $2 a_o R t_L$. Fuel members within this area are potential firebrands.

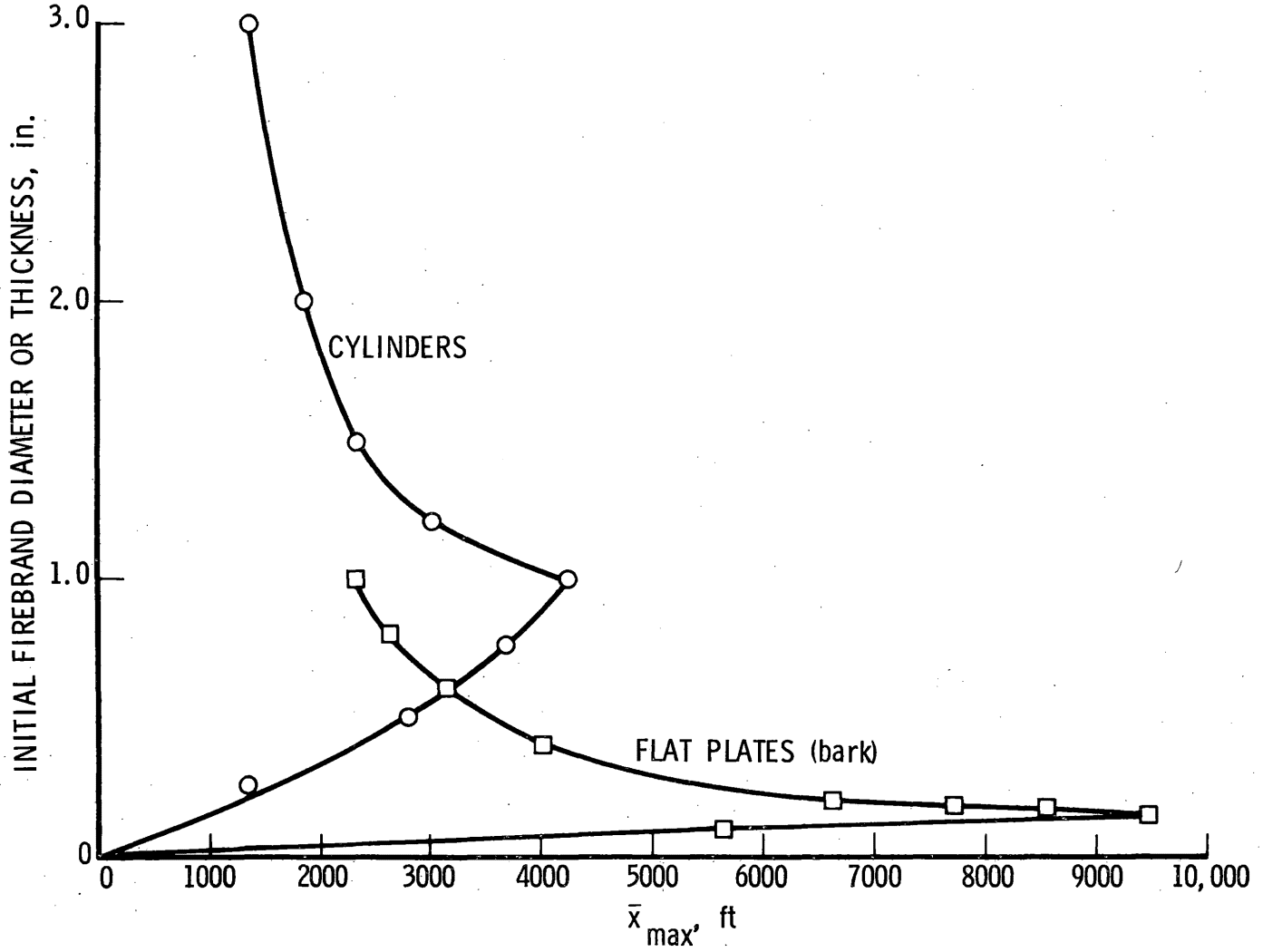

Figure 8. Maximum Firebrand Impact Distance (Without Burnout in Flight) versus Initial Firebrand Size for Logging Slash - Fire Whirl Example

The number of firebrands of a given size class that land between x_1 and x_2 is all those which are lifted from an initial position within the fire whirl between γ_1 and γ_2, as determined from Eq. (49). Fuel members of a given size are assumed to be distributed uniformly along the ground, with that fraction, given by the ratio of the area between γ_1 and γ_2 to the area of the whirl at the ground

$$\frac{\pi a_o^2\left(\gamma_2^2 - \gamma_1^2\right)}{\pi a_o^2} = \gamma_2^2 - \gamma_1^2$$

of all the fuel members of that class within an area of $2a_o Rt_L$ being potentially able to fall within x_1 and x_2. Then, the number of potential firebrands of a size class d (between d and d + Δd) that have an initial position between γ_1 and γ_2 that could be lifted during the lifetime of a fire whirl is

$$N_{d,\gamma_{1,2}} = \frac{(\Delta W_d)2a_o Rt_L\left(\gamma_2^2 - \gamma_1^2\right)}{\rho_o V_f} \tag{50}$$

where V_f is the firebrand volume and ΔW_d is the fuel loading (lb_m/ft^2) of the fuel of that size class. The number actually lifted is $F_d N_{d,\gamma_{1,2}}$. Subdividing the γ interval from $\gamma = 0$ to $\gamma = 0.1$, the x-distribution of a given size class firebrand is obtained. Considering all the pertinent size classes will enable the total number of firebrands that fall within given distances from the fire whirl to be determined. Multiplying the number of those firebrands that have $t_{res} \geq \overline{t}_{ign,g}$ by P_{ig} gives the number of spot fires created.

D. FIREBRAND GENERATION FUNCTION

The rationale for the firebrand generation function for a given size class firebrand F_d was given in Section III-D, with Eq. (21) determining F_d. For a fire whirl, much higher values of u_o/V_{cr} occur than for a convection

column. The values of K depend on the fuel and not on the lifting mechanism. For a fire whirl, reasonable values of F_d for representative sized firebrands are in the 0.01 to 0.4 range, with F_d decreasing with increasing firebrand size.

E. SPOT FIRE HAZARD

Because of the short duration and limited diameter (generally less than 50 ft), a fire whirl does not pose as severe a short-range spot fire threat as does a convection column which extends over a wide front. For instance, Appendix C-III gives an example of a plausible fire whirl for the logging slash case also considered in the convection column examples. For t_L = 100 sec, the fire whirl will cause 915 ignition points within a distance of L_3 from the front. These are spread over a width of ±200 ft (400 ft of front width). Within that same area in the same time span, the convection column would induce 16,400 spot fires. In addition, the convection column continues to generate firebrands long after the fire whirl lifetime has ended.

A fire whirl, possessing very high vertical velocities, does pose a long-range spot fire threat. Depending on the whirl intensity and vertical size, and on the wind, a fire whirl can induce spot fires several miles away. While the ignition points are few and spread out so that rapid coalescence is not a problem, they may go undetected and eventually grow into dangerous fires. These secondary fires may entrap men and equipment fighting the main fire. Also, fires which are thought to be under control can become hazardous if a fire whirl is initiated which causes long-range spotting and creates another fire that has to be contained.

For the logging slash fire whirl example, the probable number (mean expected number) of spot fires produced at distances greater than the L_3 (i.e., > 468 ft) for the associated convection column is 192, with the density of spot fires decreasing with increasing distance from the fire front (see Table C-12). The maximum threat distance is 9460 ft. This maximum

distance depends largely on the height z_e of the external swirl and on the ambient wind speed. The maximum threat distance roughly varies linearly with the wind speed and slightly stronger than linear with z_e. The number of spot fires varies linearly with F_d and P_{ig}.

The threat of long-range spot fires depends on the creation of a strong fire whirl (or other suitable lifting mechanism). The theory of Muraszew, Fedele, and Kuby [1976] shows that a viable fire whirl can exist only if the prewhirl fire intensity (the fuel mass burn rate per unit area) is sufficiently high, with a value of $\rho_b R_o = 0.01$ or $0.02\ lb_m/ft^2$-sec being the minimum required. Thus, a fire whirl is not expected to occur for the Romero example ($\rho_b R_o \sim 0.005\ lb_m/ft^2$-sec), but moderate to strong ones could occur for the logging slash example (where $\rho_b R_o = 0.14\ lb_m/ft^2$-sec).

V. SUMMARY AND CONCLUSIONS

A statistical model describing the probability of a firebrand-generated spot fire occurrence based on fire whirl or convection zone intensity, burning fuel and recipient fuel characteristics, and on meteorological and terrain conditions, was established subject to verification by laboratory tests and field observations to determine some of the key parameters of the model.

The statistical model emphasizes that the firebrand generation function, i.e., the function defining the probable number of firebrands discharged from a convection zone, is the most uncertain parameter of the model. Field data to verify and to better define it are needed.

A nominal convection column existing above the fire front is primarily responsible for the generation of a significant number of short-range (several hundred feet from the fire front) firebrands.

For short-range firebrands, criteria were established for safe-from-firebrand hazard fuel break widths and for flame coalescence ahead of the main fire front which could initiate advanced flareups. While the number of spot fires and coalescence probability depend on the firebrand generation function and on the ignition probability, the fuel break analysis does not. It depends on the conventional fire front continuous spread rate and on the in-flight and on-ground burning behavior of firebrands and is, therefore, on more firm ground.

The more powerful convection mechanism of a fire whirl contributes little, because of its limited diameter and short duration, to the short-range firebrands, but is responsible for the generation of long-range firebrands (i.e., at distances exceeding 0.5 mi) and distant spot fires.

As an example of the methodology used in the statistical model calculation, a case was presented for the Romero fire conditions (California, 1971) and for heavy logging slash (over 40 tons/acre). The main firebrand hazard in the Romero fire was found to be in the short-range firebrands, with a "safe"

fuel break of 92 ft (for 12 mph wind), and for the logging slash case both short- and long-range firebrand hazards were determined. The safe fire break width for the short-range firebrands was in that case 468 ft (with a 12 mph wind), and the maximum distance of long-range firebrands with a 6000-ft-high fire whirl was 9460 ft. The logging slash case, with a much higher dead fuel loading and higher fire spread rate than the Romero case, consequently represented a more severe spot fire hazard.

The effect of increasing wind and uphill slope is to increase the danger zone where short-range spot fires can occur and thus to increase the fuel break depth required. The maximum threat distance for long range firebrands also increases with increasing wind.

VI. RECOMMENDATIONS

A. GENERAL

Mathematical and/or statistical relationships for firebrand generation, fuel ignition, flame coalescence, convection column, and fire whirl analysis have been formulated, but their verification is not yet complete. The main future effort in wildfire research should be concentrated on an orderly collection of new field data (and review of old data not yet analyzed) and on meaningful laboratory experiments to either verify the relationship proposed or to indicate the need for revision. Generation of further sophisticated models would in all probability not improve our understanding of complex wildfire phenomenology, but would add to the delay in providing a practical and proven analytical tool to fire managers.

B. FIREBRAND GENERATION FUNCTION

Experiments to at least partially validate the firebrand generation function are needed. This can be accomplished by observations of the number of impacting firebrands resulting from a controlled test. Field observations are needed on the rate and distance of short-range firebrands produced from a fire as a function of fire front length. Simultaneous data on the fire front convection column uplift velocity at or above fuel height are also necessary. The data need not be too precise, but should be complete. For example, data such as 20 to 40 firebrands during 10 minutes in 80 to 100 ft of fire front are quite acceptable provided that the rate of fire spread, characteristics of the burning fuel (required for the Rothermel spread rate model), fraction of dead fuel and its size distribution, and ambient wind, air temperature, and humidity are also obtained. These data will also aid in assessing the appropriateness of the fuel break analysis.)

The data required can be best obtained from the observation of an actual wildfire or a controlled fire. In the latter case, fuel arrangement can be made to assure lifting of some embers.

C. FUEL IGNITION

Experimental data on the ignition of recipient fuels by flaming and glowing firebrands are needed. These data can be obtained from laboratory experiments. In such experiments, firebrands of known size and moisture content (flaming and glowing) should be dropped on recipient fuel arrays of known loading, size, type, and moisture content. Data should be obtained regarding firebrand flame or glowing surface temperature and the duration of flaming and/or glowing, the time to the recipient fuel ignition, and the process of flame spreading after ignition.

Probability of ignition data of the National Fire-Danger Rating System should be supplemented with additional data for various values of packing ratios and for the nine fuel models. These data could also be obtained in laboratory experiments with and without wind.

D. SPOT FIRE COALESCENCE

Laboratory experimental data are needed on spot fire coalescence (either radiation or normal spread-induced) of closely spaced spot fires for various fuel arrays representing the nine fuel models. The data should contain spot fire flame height, distance, fuel loading, dead fuel fraction and size distribution, and fuel moisture content. The effect of wind on flame coalescence should be included in the investigation.

E. CONVECTION COLUMN PROPERTIES

Experimental field data on convection columns are needed. The data should provide at least the uplift velocity at one or two heights and, if possible, temperatures at that height. For these data to be meaningful, all the burning fuel characteristics required for calculation of the fire spread rate by Rothermel's model should be known, and the actual fire spread rate measured or estimated. Ambient wind, air temperature, and humidity data are also required. These data can be best obtained from field measurements of controlled fires.

F. FIRE WHIRL INCEPTION

Experimental data are required on the conditions leading to the inception of ambient swirls which are one of the triggering mechanisms of a fire whirl. It is known that some combination of air temperature lapse rate, wind, and topography will lead to vortex formation. The fire itself can modify or induce external circulation. The external circulation and the rate of energy and mass release from the burning fuel are expected to determine whether or not a fire whirl is created. The quantitative assessment of the parameters involved in determining the ambient vortex intensity and its ability to start a fire whirl is needed. A laboratory experimental program providing some of this information has been previously recommended to the Forest Fire Research Laboratory in Riverside.

G. FIRE WHIRL PROPERTIES

Field measurements of naturally occurring whirls are difficult because of the special set of conditions that must be present for their formation and because of the violent and transient nature of this phenomenon. All that can be expected are photographic (movies) data from which the size of the fire whirl (diameter of the visible core and its height), the history of its motion, and its duration can be deduced. For such data to be meaningful in the verification of the proposed fire whirl model, the burning fuel characteristics needed for Rothermel's fire spread calculation must also be known. In view of the paucity of the existing data in this area, effort should be made to collect all that are available for analysis and interpretation, and to obtain new data whenever possible.

H. INSTRUMENTATION

A brief study is needed to evaluate and to categorize the best instrumentation for obtaining the data noted above. In the field tests, means for remote measurements are of prime importance.

APPENDIX A

SHORT-RANGE (CONVECTION COLUMN) FIRE HAZARD CALCULATION FLOW DIAGRAM

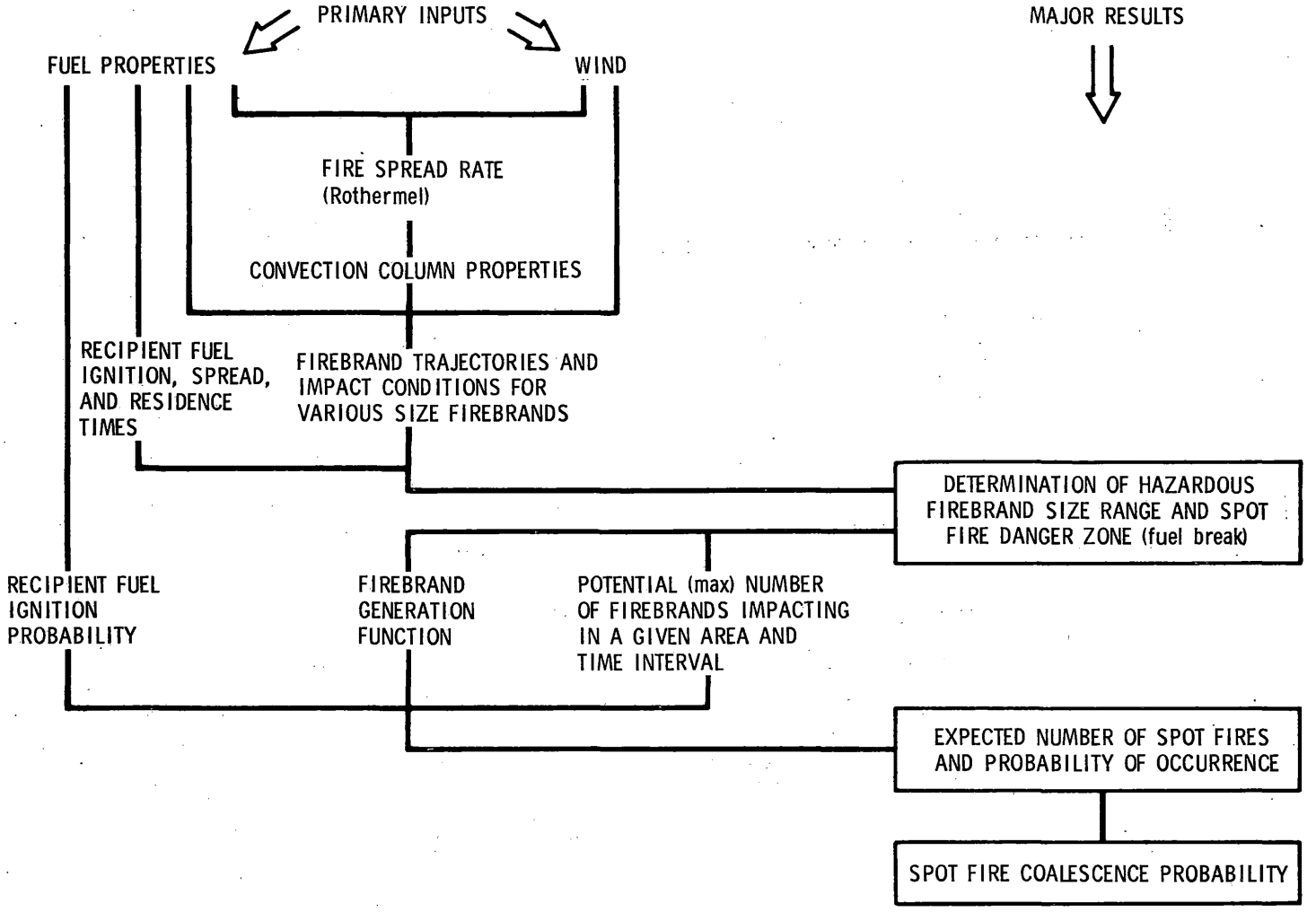

Figure A-1. Short-Range (Convection Column) Fire Hazard Calculation Flow Diagram

APPENDIX B

LONG-RANGE (FIRE WHIRL) SPOT FIRE HAZARD CALCULATION FLOW DIAGRAM

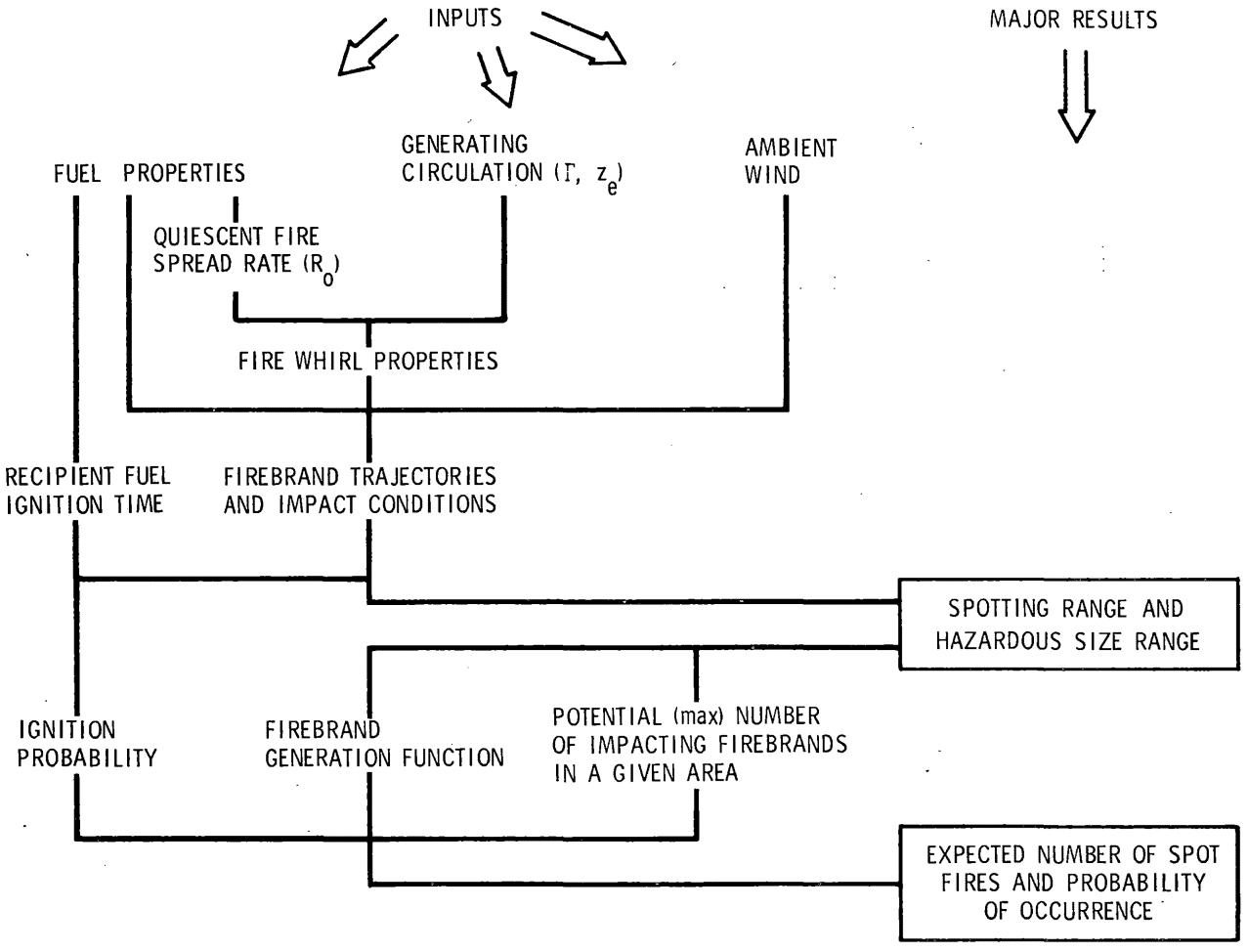

Figure B-1. Long-Range (Fire Whirl) Spot Fire Hazard Calculation Flow Diagram

APPENDIX C

EXAMPLE CALCULATIONS

APPENDIX C

EXAMPLE CALCULATIONS

I. CONVECTION COLUMN: ROMERO FIRE

The first example selects a part of the large California Romero fire, which occurred in 1971, as a typical fuel model for a convection column. The wind is taken as horizontal at 12 mph and the ground slope as zero. The fuel shape is taken to be cylindrical with L/D = 10. The dead fuel loading was 0.563 lb_m/ft^2 (12.3 tons/acre) with mean diameter of 0.433 cm and mean moisture content of 2 percent. The cumulative dead fuel loading distribution versus diameter is given in Figure C-1. The total fuel loading was 1.604 lb_m/ft^2 (35 tons/acre) with mean diameter of 0.263 cm and mean moisture content of 33 percent. The mean fuel density was 46.7 lb_m/ft^2, with the packing ratio $\beta = 0.005$; β_{op} and R, as determined from the Rothermel formulation, were 0.02 and 73.01 ft/min, respectively.

The convection column properties for this case are obtained using the formulation given in Section III-C. From Eqs. (9) through (14), u_o = 43.77 ft/sec; ℓ = 124 ft; b_g = 5.21 ft; and $\rho_f \ell$ = 0.0266 lb_m/ft^3. The tilt of the column due to wind as given by Eq. (17) is ϕ = 21.9 deg.

The first steps in determining the spot fire hazard are to calculate L_1 and L_3. The L_1 is determined by Eq. (23), with $\bar{t}_{spr}$ and $\bar{t}_{ign}$ given by Eqs. (22) and (3), respectively.

$$t_{spr} = 43.3\ (0.433)^2\ \ell n\ \frac{0.950}{0.005} = 42 \text{ sec}$$

The $\bar{t}_{ign} = 17.5\ (0.433)^{0.75} = 9.34$ sec, and from trajectory calculations, utilizing the above convection column properties, t_f was found to be about 3 sec. Thus

$$L_1 = \frac{73.01}{60}\ [3 + 9.34 + 42] = 66 \text{ ft}$$

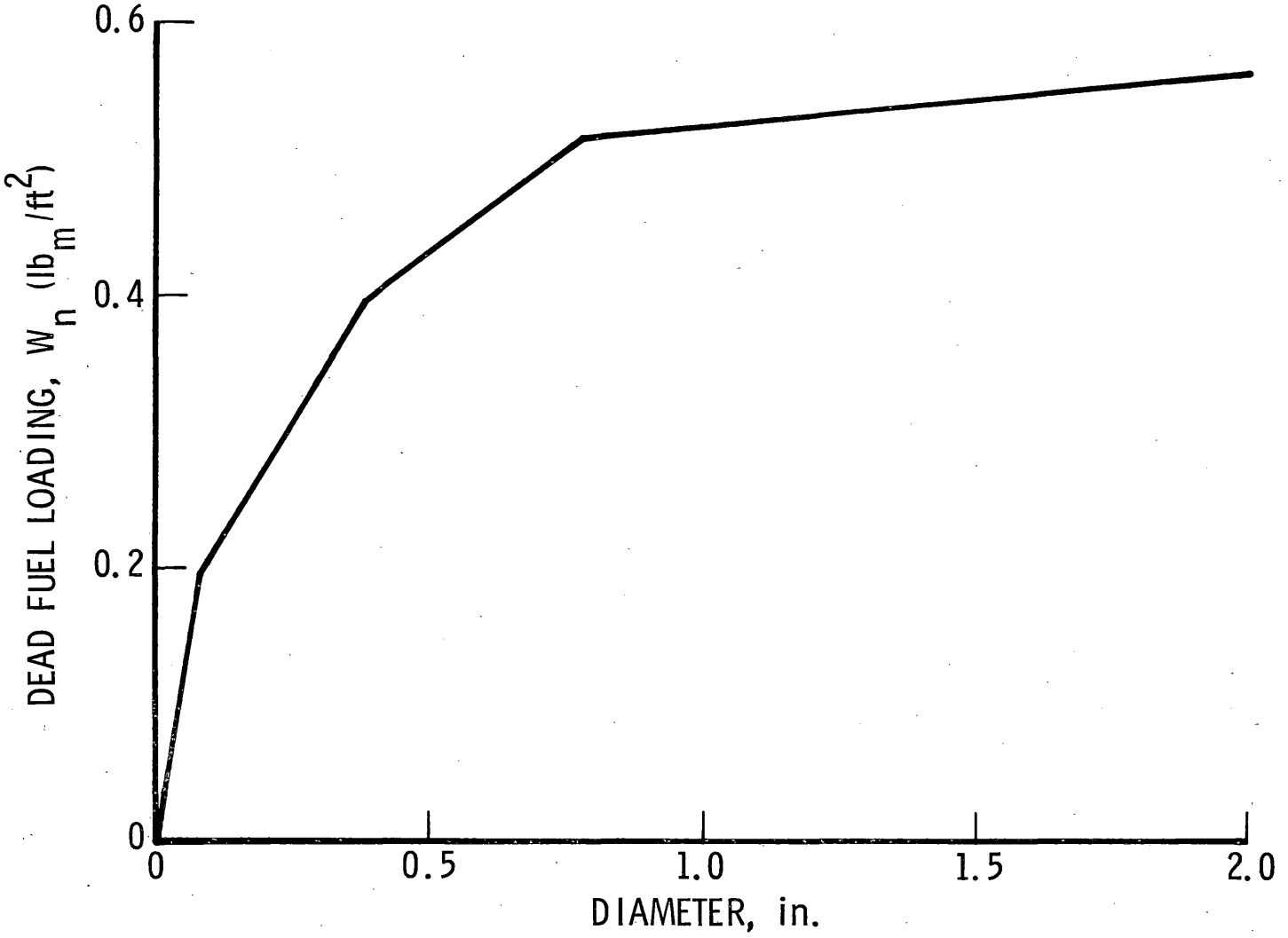

Figure C-1. Cumulative Dead Fuel Loading (W_n) versus Diameter for Romero Fire

The maximum threat distance for a given size firebrand L_{max} is found from the firebrand impact conditions. For a given size firebrand, the maximum travel distance ℓ_{x_d} (without being burned out in flight) and the threat distance [maximum travel distance with $\rho_{imp} \geq \rho_{cr}$ where ρ_{cr} is determined by Eq. (24)] are determined from the trajectory and firebrand burning equations. These results are shown in Table C-1. This table gives the relative position in the column at liftoff, the maximum travel distance ℓ_{x_d}, the impact density ratio, the critical impact density ratio, and L_{max}, the threat distance for various firebrand diameters. For a particular size of firebrand, the distance L_{max} will be greatest and that distance is identified as L_3 (Figure C-2).

As seen from Table C-1, a $D_o = 0.256$ cm firebrand has the greatest L_{max}, 92 ft. Anything bigger has a smaller maximum travel distance. Firebrands greater than $D_o = 0.293$ will travel less than 66 ft and, since $L_1 = 66$ ft, they will not be a threat. The $D_o = 0.256$ cm firebrand impacts with $\rho_{imp} = \rho_{cr}$. A lighter firebrand could travel further (a greater ℓ_{x_d}) but will land with $t_{res} < \bar{t}_{ign}$ ($\rho_{imp} < \rho_{cr}$) and, hence, would not be a threat. For instance, a $D_o = 0.244$ cm firebrand, if it is lifted at the extreme upwind edge of the column ($x(0)/b_g = -1$), will travel 111 ft from the fire front, but will land with a density ($0.17\rho_o$) less than the critical ($0.25\ \rho_o$), and, thus, is not a threat. If its initial liftoff location is moved downwind, a location is reached ($x(0)/b_g = -1/5$) so that its impact density equals ρ_{cr}. This is because the firebrand will not stay in the column as long and will not be lifted as high into the column. The travel distance for this particular firebrand is just equal to L_1 (66 ft).

Table C-1 also gives the maximum impact distance (largest ℓ_{x_d}) as 135 ft, and this is for $D_o = 0.232$ cm. Here, the firebrand is just on the verge of burning out in flight when it lands, and $\rho_{imp} < \rho_{cr}$. Not until $x(0)/b_g = 0.5$ will it land with $\rho_{imp} = \rho_{cr}$, and then it falls within L_1, and is thus not a threat.

Table C-1. Firebrand Trajectory and Impact Characteristics, Romero Fire

D_o		$x(0)/b_g$	ℓ_{x_d}	ρ_{imp}/ρ_o	ρ_{cr}/ρ_o	L_{max}
cm	in.					
0.232	0.091	-1	135	0.05	0.35	--
0.232	0.091	1/2		0.35		47
0.244	0.096	-1	111	0.17	0.25	--
0.244	0.096	-1/5		0.25		66
0.256	0.101	-1	92	0.19	0.19	92
0.293	0.115	-1	66	0.41	0.11	66

L_3 = greatest L_{max} = 92 ft

Limiting firebrand size for lifting, D_o = 0.790 cm (0.31 in.)

The trajectory results are also shown in Figure C-2, where L_{max}, ℓ_{x_d}, ρ_{imp}/ρ_o at $x = \ell_{x_d}$, and ρ_{cr}/ρ_o are given. Note that $L_{max} = \ell_{x_d}$ for any D_o for which $\rho_{imp} \geq \rho_{cr}$ (i.e., for $D_o \geq 0.256$ cm). For smaller firebrands, $L_{max} < \ell_{x_d}$.

The threat zone extends from L_1 to L_3 (from 66 to 92 ft) ahead of the instantaneous fire front location. Thus, a fuel break has to be greater than 66 ft to be of any use, and 92 ft is required to remove the short-range spot fire threat.

Firebrands of diameter of approximately 0.25 to 0.29 cm are spot fire threats. For this small range, it is not necessary to subdivide the size interval, but it suffices to consider a single size class. From Figure C-1, the weight of dead fuel in this size range ΔW_d can be obtained. From Eq. (1), the potential liftoff rate of firebrands, per foot of front, is determined as

$$N_d = \frac{4(0.01)(73.01)/60}{(3.14)(10)\left[\frac{0.25}{(30.48)}\right]^3(46.7)} = 60.8/\text{ft/sec}$$

The rate per foot of front actually lifted is $F_d N_d$, where F_d is given by Eq. (21). The value of K for the Romero fuel model is taken to be 0.001, so that $F_d = 0.0021$. The rate at which firebrands land per square foot is $F_d N_d / \ell_{x_d} = 0.0021(60.8)/92 = 0.00139$ per ft^2 per sec. The number of spot fires per square foot in the danger zone is $P_{ig} F_d N_d / \ell_{x_d}$. The weather conditions are taken as sunny with a temperature of 75°F. Then, from Table 1 of the text, $P_{ig_o} = 0.9$. With $\beta/\beta_{op} = 0.005/0.02$, $P_{ig}(\beta/\beta_{op}) = 0.225$. Then, there are $0.225(0.00139) = 0.000313$ spot fires/sec-ft^2 in the danger zone. Per hundred feet of front, there are 48.8 spot fires started per minute within the 26-ft deep danger zone.

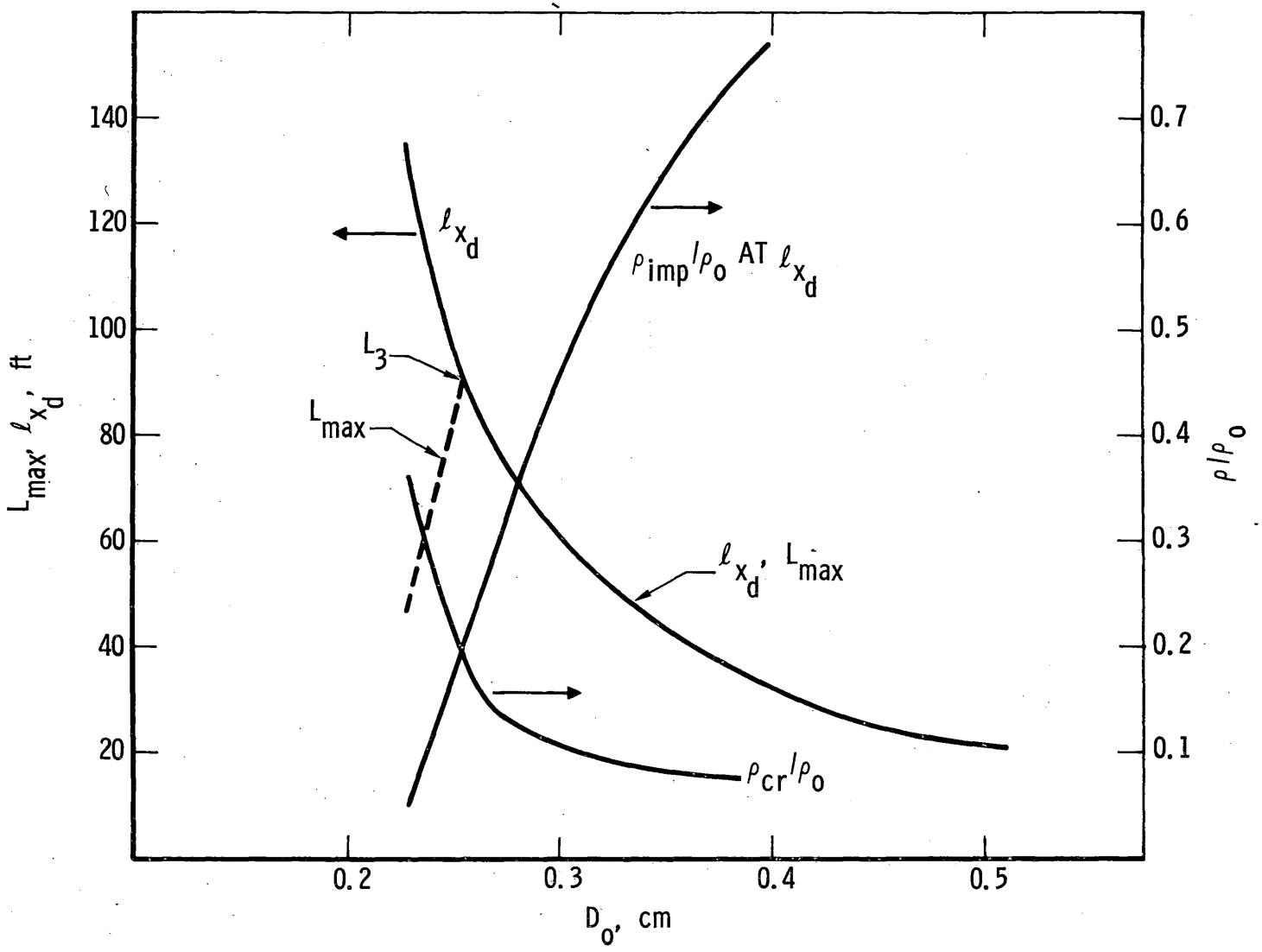

Figure C-2. Firebrand Density and Maximum Travel Distance at Impact (ℓ_{x_d}) and Threat Distance (L_{max}) versus Diameter, Wind = 12 mph (Romero example)

The probability that coalescence will occur within the danger zone per 100 ft of front width is given by Eqs. (25) and (29), with t_{resid} (which is based on the mean size and moisture content of all the fuel, both live and dead), being given by Eqs. (5) through (7)

$$t_{resid} = 43.3(0.263)^2 \left(\frac{33}{2}\right)^{0.44} \ell_n \frac{0.95}{0.005} = 53.9 \text{ sec}$$

The required view factor is

$$\frac{1.4Q_i}{2t_{resid}q_r} = \frac{1.4(14)}{2(53.9)0.25} = 0.73$$

From the Keith [1962] view factor graphs, with a flame height equal to the fuel bed depth of 7.5 ft and the flame inclined 30 deg from the vertical, the maximum distance for spontaneous ignition of the median strip between two spot fires (h_{cr}) is 2 ft. Then the expected, or most probable, number of spot fires within an area (1) Yh_{cr} within a time t_{resid} is [from Eq. (25)]

$$\lambda = P_{ig}F_dN_dYh_{cr}t_{resid}/\ell_{x_d}$$

$$= 0.000313\ Yh_{cr}t_{resid} = 0.0337Y$$

where Y is the number of spot fires needed to coalesce.

Equation (29) then gives the probability of coalescence for any value of Y, A, and t. Within the danger zone, per 100 ft of front, $A = 26(100) = 2600 \text{ ft}^2$. (This danger zone is relative to the instantaneous front location, and moves forward with the fire front.) The probability of coalescence of Y spot fires within a time t (per 100 ft of front) is given in Table C-2 for various values of Y and t. Thus, for instance, the probability of rapid coalescence of four spot fires within one hour is 23.3 percent.

Table C-2. Probability of Coalescence of Y Spot Fires within a Time t, Romero Fire (t_{resid} = 53.9 sec, h_{cr} = 2 ft)

Y	t, min	λ	P ($\geq$Y)
5	1	0.1681	0.000282
	15	0.1681	0.00433
	30	0.1681	0.00841
	60	0.1681	0.0168
4	1	0.1345	0.00442
	15	0.1345	0.0643
	30	0.1345	0.124
	60	0.1345	0.233
3	1	0.1009	0.0737
	15	0.1009	0.683
	30	0.1009	0.899
	60	0.1009	0.990

Note: The number of spot fires in the danger zone (L_3-L_1 = 26 ft) is 48.8 per 100 ft of fire front.

The quantities h_{cr} and t_{resid} appear as a product in λ and in Eq. (29). Thus, a change in h_{cr} is equivalent to a change in t_{resid}. The change in coalescence probability with h_{cr} (or with t_{resid}) is shown in Table C-3.

The quantities P_{ig} and F_d appear as a product. While the number of spot fires depends linearly on the product $P_{ig}F_d$, the probability of coalescence is a strong function of λ, and hence of $P_{ig}F_d$. Table C-4 gives the sensitivity of the coalescence results to F_d (or to K) for Y = 4, h_{cr} = 2 ft. It then equivalently indicates the sensitivity to P_{ig}. The uncertainty in the true value of F_d is expected to be much larger than the uncertainty in P_{ig}. The smaller the value of P ($\geq$Y), the larger the change in P for a given change in F_d (or P_{ig}).

The preceding results were based on a 12 mph wind speed and a zero ground slope. The depth of the danger zone is dependent on both wind and ground slope. An increase in the wind and the uphill ground slope will increase the fire front spread rate R, resulting in a higher convection column uplift velocity. The effect of changes in wind and slope are shown in Table C-5, where results for R, u_o, max (ℓ_{x_d}), $D_{\ell_{max}}$ (the diameter of the firebrand which has the maximum ℓ_{x_d}), L_1, L_3, and D_{L_3} (the diameter of the firebrand which has the greatest threat distance) are given. The wind is taken to be parallel to the ground in all cases, so that there are horizontal and vertical wind components for the slope case.

Table C-5 shows the increase in L_1 and L_3 with wind and slope. Firebrand travel distances depend directly on the wind. The L_3 depends directly on R and L_1 indirectly (since u_o depends on R), and R increases with wind and with slope. The rate of increase of R with wind depends directly on the fuel characteristics, namely the fuel packing ratio and mean fuel diameter. The rates of change for a specific case can be obtained from the Rothermel [1972] formulation for R.

Table C-3. Effect of h_{cr} (or t_{resid}) on Romero Fire Coalescence Probability (t_{resid} = 53.9 sec), for Coalescence within Time t

h_{cr}, ft	t	P (≥4)
2	15 min	0.064
	30 min	0.124
	1 hr	0.233
5	15 min	0.587
	30 min	0.830
	1 hr	0.971
7	15 min	0.888
	30 min	0.987
	1 hr	0.999
For Y = 4		

Table C-4. Effect of F_d (or K) on Romero Fire Coalescence Probability (h_{cr} = 2; t_{resid} = 53.9 sec)

K	F	t	P (≥4)
0.0005	0.001	15 min	0.00361
		30 min	0.00720
		1 hr	0.0144
0.001	0.0021	15 min	0.0643
		30 min	0.124
		1 hr	0.233
0.002	0.0042	15 min	0.615
		30 min	0.852
		1 hr	0.978
For Y = 4			

Table C-5. Effect of Wind and Slope on the Danger Zone Characteristics (Romero Fire)

slope, deg	0	0	45
wind, mph	12	20	12[a]
R, ft/min	73	104	110
u_o, ft/sec	43.8	49.2	50.2
max (ℓ_{x_d}), ft	135	220	255[a]
$D_{\ell_{max}}$, cm	0.232	0.238	0.287
L_1, ft	66	94	100[a]
L_3, ft	92	161	199[a]
D_{L_3}, cm	0.256	0.262	0.305

[a]measured parallel to the ground

II. CONVECTION COLUMN: LOGGING SLASH EXAMPLE

The second example is for a typical logging slash area, with a wind of 12 mph and a zero ground slope. The fuel is all dead fuel with a heavy loading of 43.1 tons/acre. The fuel consists of foliage (e.g., small needles), cuttings, bark, etc. The foliage, being very small in size, burns up quickly and is not a firebrand threat. The remaining material is taken to be both cylindrical and flat plate (bark) in shape, with 23 percent of the material up to 1 in. in size (diameter or thickness) being bark. Table C-6 gives all of the pertinent fuel characteristics, including the weight-size distribution.

The convection column properties are calculated to be: $u_o = 67.6$ ft/sec; $\ell = 295.5$ ft; $b_g = 3.52$ ft; $\rho_{f\ell} = 0.0266$ lb_m/ft^3; $\phi = 14.6$ deg. The fire spread rate calculated from Rothermel's [1972] formula for 12 mph wind was 214.6 ft/min.

The fuel break analysis is as follows:

$$\bar{t}_{spr} = 43.3(0.125)^2(2.5)^{0.18}\,\ell n\left(\frac{0.95}{0.005}\right) = 5.35 \text{ sec}$$

$$\bar{t}_{ign} = 17.5(0.125)^{0.75}(2.5)^{0.44} = 4.3 \text{ sec}$$

$$t_{f\ell} \sim 2.5 \text{ sec (from trajectory calculations)}$$

therefore

$$L_1 = \frac{214.6}{60}[2.5 + 4.3 + 5.4] \cong 44 \text{ ft}$$

The maximum threat distance L_3 is found from trajectory calculations. In this case, the minimum size fireband that is a threat is found to be the one which can just escape from the column. Any smaller size than 0.725 cm is not able to leave the column, irrespective of its location within the column,

Table C-6. Fuel Characteristics for Logging Slash Example

Weight-Size Distribution	
Size (diameter, thickness)	tons/acre
foliage	21.8
0 to 0.25 in.	8.8
0.25 to 1 in.	10.5
1 to 3 in.	2.0
	43.1

$\overline{d}$ = 0.125 cm, δ = fuel bed height $\cong$ 2.5 ft

L/D, L/H = 10

β = 0.03, β_{op} = 0.012, W_n = 2 lb_m/ft^2, M = 5 percent

ρ_b = 0.75 lb_m/ft^3, ρ_o = 25 lb_m/ft^3

R_o = 11 ft/min, R = 214.6 ft/min

$\rho_b R_o$ = 0.14 lb_m/ft^2 - sec

because the angle between the firebrand velocity vector and the vertical is less than the slope of the convection column. (In reality, a small size firebrand would be able to leave the column after traveling sufficiently high up, except that it would remain in the column long enough to be consumed by the fire.) All sizes have $L_{max} = \ell_{x_d}$ (i.e., all have $\rho_{imp} > \rho_{cr}$). Thus, this smallest size has both the maximum value of ℓ_{x_d} and of L_{max}. The largest size that needs to be considered is that which has an ℓ_{x_d} equal to L_1.

Table C-7 gives the values of ℓ_{x_d}, N_d, F_d, t_c (time of flight within the column), and t_t (total time of flight) for sizes from the minimum to the maximum, for both cylindrical and bark-like firebrands. The values of F_d were obtained by taking K = 0.00335. This results in $F_d = 0.01$ when $u_o/v_{cr} = 2$. Note that this value of K is more than three times greater than for the Romero example. The logging slash case has more unattached fuel members with little overhead cover, and thus warrants a larger value of K. The values of F_d are then also correspondingly larger, due to the larger K and the larger value of u_o.

The weather conditions are taken to be sunny with a temperature of 80^oF. Then, from Table 1 of the text, $P_{ig} = 0.61$ (for M = 5 percent). ($P_{ig} = P_{ig_o}$ since $\beta/\beta_{op} > 1$.)

The danger zone ($L_1 < x < L_3$) is large. For cylindrical firebrands, it is 468 - 44 = 424 ft deep. For the bark, it is 440 - 44 = 396 ft deep. The danger zone is subdivided into subzones. The firebrand size range of interest, for both cylindrical and plate-like firebrands, is also divided into subintervals of five size classes each. The total number of expected spot fires occurring in a given subzone of depth ΔL_x, per 100 ft of fire front in one minute, is equal to $P_{ig} (\Sigma F_d N_d/\ell_{x_d}) 60 \cdot 100 \cdot \Delta L_x = N_s$, where the sum is over size classes for both cylinders and plates. The characteristic size for the classes is as indicated in Table C-7, varying from 0.725 to 1.158 cm for cylindrical firebrands, etc. Then, with ΔW_d determined from Table C-6 (assuming a linear cumulative weight versus size distribution function within the size ranges given in Table C-7) and N_d from Eq. (1), N_s can be determined.

Table C-7. Firebrand Characteristics for Logging Slash Example

Cylindrical Firebrands						
D		ℓ_{x_d}, ft	N_d, 1/ft-sec	F_d	t_c, sec	t_t, sec
cm	in.					
0.725	0.285	468	0.031	0.0128	7.8	27.0
0.780	0.307	273	0.057	0.0116	5.1	15.9
0.853	0.336	176	0.084	0.0104	3.6	10.4
0.945	0.372	116	0.219	0.0091	2.6	7.0
1.158	0.456	63	0.188	0.0068	1.7	4.0
1.341[a]	0.528	44	--	--	--	--
L_3 = 468 ft Limiting size for lifting, D_o = 3.51 cm (1.38 in.)						
Flat-Plate (Bark) Firebrands						
H		ℓ_{x_d}, ft	N_d, 1/ft-sec	F_d	t_c, sec	t_t, sec
cm	in.					
0.570	0.224	440	0.0029	0.0128	7.8	25.4
0.610	0.240	276	0.0037	0.0118	5.3	16.1
0.671	0.264	172	0.0028	0.0104	3.6	10.2
0.732	0.288	121	0.0091	0.0093	2.7	7.3
0.914	0.360	63	0.0059	0.0067	1.7	4.0
1.036[a]	0.408	44	--	--	--	--
L_3 = 440 ft Limiting size for lifting, H = 2.76 cm (1.08 in.)						

[a]None of this size lands within $L_1 < x < L_3$.

Table C-8 gives N_s within the total danger zone, for each of six subzones. The probable number of spot fires occurring in one minute per 100 ft of front is 2460. For the Romero case, there were about 49. The logging slash case, with its higher dead (and total) fuel loading and fuel mass burn rate, constitutes a much greater spot fire threat than does the Romero case. The danger zone depth is larger by over a factor of 15 (a larger fuel break is thus required) and the probable number of spot fires is also much larger.

To determine the probability of coalescence, t_{resid} and h_{cr} are needed. Since all the fuel is dead, $t_{resid} = \bar{t}_{spr} = 5.35$ sec. The h_{cr} required by the usual radiation flux-induced spontaneous ignition procedure is very low due to the low values of fuel depth and t_{resid}. In this case, rapid coalescence will occur because of the natural growth of two adjacent fires rather than by radiation heating of the ground between them. Two adjacent fires will, in a time of t_{resid}, each travel a distance of $t_{resid}R_o$ in a direction normal to the wind where R_o is the fire spread rate with no wind and zero slope. Thus, $h_{cr} = 2R_o t_{resid} = 2(11/60)5.35 = 2$ ft. The probability of coalescence of four spot fires ($Y = 4$) within various time periods within each of the six subzones is given in Table C-9. The probability that coalescence of four spot fires will occur within one hour per 100 ft of front anywhere in the entire danger zone ($L_1 < x < L_3$) is 99.97 percent. This compares with a value of 23.3 percent for the Romero example. Since the rate of spot fire initiation per ft^2 decreases with increasing distance from the fire front, the probability of coalescence also decreases. In particular, the coalescence probability in subzones 1 and 2 (the two farthest from the fire front), located from 275 to 468 ft from the instantaneous front, is very small. For instance, even within 1000 ft of front width, the probability of coalescence of four spot fires in subzone 1 occurring anytime within one hour is about 0.1 percent, and in subzone 2, about 1 percent. Thus, while a fuel break of 468 ft deep is needed

Table C-8. The Total Number of Expected Spot Fires within ΔL_x within One Minute per 100 ft of Front Width (Logging Slash Example)

Subzone Number	L_x, ft	ΔL_x, ft	N_s
1	468-440	28	41
2	440-275	165	262
3	275-175	100	417
4	175-120	55	413
5	120- 63	57	858
6	63- 44	19	469
$\Sigma N_s = 2460$			

Table C-9. Probability of Coalescence of Four Spot Fires in Each Subzone per 100 ft of Front (Logging Slash Example)

Subzone Number	Time Period			
	1 min	15 min	30 min	1 hr
1	0.000002	0.000028	0.000056	0.00011
2	0.0000016	0.00024	0.00047	0.00095
3	0.000446	0.00668	0.0133	0.0264
4	0.00252	0.0371	0.0729	0.1404
5	0.0399	0.457	0.705	0.913
6	0.0882	0.750	0.937	0.996

Probability of coalescence of four spot fires occurring within one hour in any of the six regions =

$$1 - \prod_{i=1}^{6} [1 - P_i(\geq 4)] = 0.9997$$

to eliminate the short-range spot fire threat, a break of 275 ft will greatly reduce the probability of rapid coalescence occurring. Of course, as seen from Table C-8, there are still 41 and 262 individual spot fires occurring within one minute per 100 ft of front in regions 1 and 2, respectively, and these individual spot fires can still be dangerous even if rapid coalescence does not occur.

III. FIRE WHIRL: LOGGING SLASH EXAMPLE

As discussed in the text, a strong fire whirl requires an intense fire for initiation, one having a value of $\rho_b R_o$ of at least 0.01 to 0.02 lb_m/ft^2-sec. The Romero fire does not qualify, but the logging slash example has $\rho_b R_o$ = 0.14 lb_m/ft^2-sec. A viable fire whirl is thus plausible for the logging slash case. Table 3 of Muraszew, Fedele, Kuby [1976] gives solutions for values of $\bar{d}$ and $\rho_b R_o$ close to those of the logging slash case. Taking Γ and z_e to be 6000 ft^2/sec and 6000 ft, respectively, then u_o = 300 ft/sec, a_o = 12 ft are reasonable. The wind is again taken to be 12 mph.

The fuel characteristics have been given in Table C-6. The trajectory calculations have been computerized. Results for cylindrical and bark firebrands are shown in Table C-10. Table C-10 gives $\bar{x}_{max}$, t_w (the firebrand in-flight burning time), ρ_{imp}/ρ_o, and D_{imp}/D_o versus D_o for cylinders and versus H (thickness) for flat plates. (For flat plates, $H_{imp} \sim H_o$.) The smallest sizes considered are limited by the in-whirl burnout criteria (see Section IV-C) and the largest by the largest fuel sizes available. For the cylinders, the ranges of the three smallest sizes are limited due to in-flight burnout (defined as occurring when either $\rho/\rho_o < 0.05$ or $D/D_o < 0.05$). The ranges of the two smallest bark sizes are likewise limited. Table C-10 shows that the maximum range is much greater for the bark (9460 ft) than for the twigs or cylinders (4250 ft). This is because plates burn slower than cylinders and, hence, the smaller sizes of bark can travel further before they burnoout. (Note that the in-flight burning time t_w is much larger for the plates.)

Table C-10. Impact Properties of Firebrands (Logging Slash Fire Whirl Example)

Cylinders				
D_o, in.	$\bar{x}_{max}$, ft	t_w, sec	ρ_{imp}/ρ_o	D_{imp}/D_o
0.25	1338	76	0.05	0.227
0.50	2825	160.5	0.20	0.05
0.66	3670	208.5	0.30	0.05
1	4250	241.5	0.50	0.14
1.2	3010	171	0.66	0.44
1.5	2323	132	0.79	0.68
2	1813	103	0.90	0.88
3	1346	76.5	0.97	0.98

Flat Plates			
H, in.	$\bar{x}_{max}$, ft	t_w, sec	ρ_{imp}/ρ_o
0.1	5650	321	0.05
0.15	9460	537.5	0.05
0.162	8545	485	0.21
0.174	7700	437.5	0.33
0.2	6644	377.5	0.50
0.4	4039	229.5	0.87
0.6	3150	179	0.93
0.8	2649	150.5	0.96
1.0	2314	131.5	0.97

The number of potential firebrands of a given size class (the size classes chosen correspond to the sizes in Table C-10) initially located between γ_1 and γ_2 in the whirl is given by Eq. (50). The number actually lifted is $F_d N_{d,\gamma_{12}}$, and the resulting number of spot fires is obtained by multiplying those firebrands which land for which $t_{res} \geq \bar{t}_{ign,g}$ by P_{ig}. From Eqs. (30) and (31), $\bar{t}_{ign,g} = 2.75$ sec. Since $\bar{t}_{ign,g} < \bar{t}_{ign} = 4.3$ sec, $\bar{t}_{ign}$ is used as the ignition time. With this small a value of $\bar{t}_{ign}$, almost all firebrands which land will have $t_{res} \geq \bar{t}_{ign}$. For instance, the smallest size cylindrical firebrand ($D_o = 0.25$ in.) has $\rho_{imp}/\rho_o = 0.559$, which is very close to the in-flight burnout value of 0.05. Thus, the $t_{res} \geq \bar{t}_{ign,g}$ ($t_{res} \geq \bar{t}_{ign}$ for this case) requirement does not limit the number of spot fires for this case. As for the convection column calculations, $P_{ig} = 0.61$, and F_d is given by Eq. (21), with again K = 0.00335 for the logging slash fuel model.

The values of F_d, $N_{d,\gamma_{1,2}}$, and $N_{s_{d,\gamma_{1,2}}}$ (the number of spot fires due to a given size class firebrand initially located within γ_1, γ_2 produced during the lifetime of the fire whirl) for selected size classes within various $\Delta\gamma$ is given in Table C-11 for bark firebrands. Also given are the $\bar{x}$ associated with the γ ranges. The fire whirl lifetime t_L is taken to be 100 sec. Results for the other size classes of interest and for cylindrical firebrands were also calculated but are not shown here. The firebrand generation function F_d is much larger here than for the associated convection column, due to the much larger value of u_o for the fire whirl. The distances $\bar{x}$ shown in Table C-11 are calculated according to Eq. (49).

The total mean probable number of spot fires induced during the lifetime of the fire whirl (100 sec) is 1107. The breakdown as to how many are generated within various distances from the fire front is given in Table C-12. The lateral spread (normal to x) of the threat corridor is approximately 400 ft, as given in Section IV-C. As discussed in Section IV-E, the short-range spot fire threat from the fire whirl is much less than from the convection column.

Table C-11. Spot Fires at Various Distances Induced by Selected Sizes of Firebrands (Logging Slash Fire Whirl Example)

H, in.	γ	$\bar{x}$, ft	F_d	$N_{d,\gamma_{1,2}}$	$N_{s_{d,\gamma_{1,2}}}$
0.1	0-0.01	5650	0.36	12.43	2.5
	0.01-0.03	5650-1502		99.4	19.5
	0.03-0.06	1502-465		335.6	65.5
	0.06-0.1	465-50		795.5	155.5
0.15	0-0.01	9460	0.26	0.79	0.12
	0.01-0.03	9460-2490		6.29	1.0
	0.03-0.06	2490-747		21.21	3.4
	0.06-0.1	747-50		50.3	8.0
0.2	0-0.01	6644	0.20	3.03	0.37
	0.01-0.03	6644-1760		24.23	0.96
	0.03-0.06	1760-538		81.78	9.98
	0.06-0.1	538-50		193.84	23.65
0.4	0-0.01	4039	0.10	0.27	0.016
	0.01-0.03	4039-1084		2.20	0.13
	0.03-0.06	1084-345		7.42	0.45
	0.06-0.1	345-50		17.58	1.07

Table C-12. Total Number of Spot Fires Induced within Various Distances from the Fire Front (Logging Slash Fire Whirl Example)

Distance from Front, ft	Number of Spot Fires
<468	915
468-1000	114
1000-1500	40
1500-3000	19
3000-5500	14
5500-9460	5
Total Number = 1107	
Total for $\bar{x}$ > 468 ft = 192	

The probability of coalescence due to the fire whirl is essentially nil. Thus, the main threat is from individual long-range spot fires that start a large distance away from the main front. If they go unobserved and become large fires, they can become a threat to men and equipment fighting the main front. The probability that at least one spot fire will be generated during the fire whirl's lifetime is very nearly one. For instance, the probability that at least one spot fire will occur within 5500 ft $< X <$ 9460 ft is 0.9975; [$P(\geq 1) = 1 - P(0) = 1 - \exp(-5) = 0.9933$]. The probability that at least three will occur is

$$P(\geq) = 1 - P(0) - P(1) - P(2) = 1 - (1 + 5 + 5^2/2) \exp(-5) = 0.88$$

The probability that at least six will occur is 0.39, and $P(\geq 7) = 0.24$.

REFERENCES

Anderson, H. E. [1968], "Sundance Fire: An Analysis of Fire Phenomena," Research Paper INT-56, USDA Forest Service, Intermountain Forest and Range Experiment Station, Ogden, Utah, 39 pp.

Anderson, H. E. [1969], "Heat Transfer and Fire Spread," Research Paper INT-69, USDA Forest Service, Intermountain Forest and Range Experiment Station, Ogden, Utah.

Anderson, H. E. and Dwight S. Stockstad [1973], "Report on the Investigation of Ignition of Fuels from the Vicinity of the West Branch Elk Creek Fire, Medford, Oregon, August 8, 1972," USDA Northern Forest Fire Laboratory internal communication, 7 pp.

Berlad, A. L. [1970], "Fire Spread in Solid Fuel Arrays," Combustion and Flame, 14.

Blackmarr, W. H. [1972], "Moisture Content Influences Ignitability of Slash Pine Litter," Research Note SE-173, USDA Forest Service.

Bunting, Stephen C. and Henry A. Wright [1973], "Ignition Capabilities of Non-Flaming Firebrands," 14-22-73, Department of Range and Wildlife Management, Texas Technological College, Lubbock, Texas.

Byram, G. M. and R. E. Martin [1970], "The Modeling of Fire Whirlwind," Forest Science, 16(4), pp. 386-399.

Cheney, N. P. and G. A. V. Bary [1969], Forest Research Institute, Canberra, Australian Capital Territory.

Countryman, C. M. and C. W. Philpot [1970], "Physical Characteristics of Chamise as a Wildland Fuel," Research Paper PSW-66, USDA Forest Service.

Keith, F. [1962], Radiation Heat Transfer, International Textbook Co., Scranton, Pennsylvania.

Martin, S. [1964], "Ignition of Organic Materials by Radiation," Fire Research Abstracts and Review, 6.

Morton, B. R. [1956], "Turbulent Gravitational Convection from Maintained and Instantaneous Sources," Proceedings of Royal Society of London, 234, pp. 1-22.

Muraszew, A. [1974], "Firebrand Phenomena," Report No. ATR-74(8165-01), The Aerospace Corporation, El Segundo, California, 109 pp.

Muraszew, A., J.B. Fedele and W.C. Kuby [1975], Report No. ATR-75(7470)-1, "Firebrand Investigation," The Aerospace Corporation, El Segundo, California, 104 pp.

Muraszew, A., J.B. Fedele and W.C. Kuby [1976], "Investigation of Fire Whirls and Firebrands," Report No. ATR-76(7509)-1, The Aerospace Corporation, El Segundo, California, 155 pp.

"National Fire-Danger Rating System (rev) [1974], Research Paper RM-84, USDA Forest Service, Rocky Mountain Forest and Range Experiment Station, Fort Collins, Colorado.

Putnam, A.A. [1965], "A Model Study of Wind-Blown Free Burning Fires," Tenth Symposium on Combustion, 1964, The Combustion Institute.

Rothermel, R.C. [1967], "Sundance Fire," Eastern States Section, The Combustion Institute, 4 pp.

Rothermel, R.C. [1972], "A Mathematical Model for Predicting Fire Spread in Wildland Fires," Research Paper INT-115, USDA Forest Service, 40 pp.

Rothermel, R.C. and Charles W. Philpot [1973], "Predicting Change in Chaparral Flammability," Northern Firest Fire Laboratory, Missoula, Montana.

Schneider, P.J. [1963], Temperature Response Charts, John Wiley and Sons, New York, New York.

Simms, D.L. [1960], "Ignition of Cellulosic Materials by Radiation," Combustion and Flame 4(4), December.

Simms, D.L. [1963], "On the Pilot Ignition of Wood by Radiation," Combustion and Flame, 7, p. 253.

Simms, D.L. and M. Law [1967], "The Ignition of Wet and Dry Wood by Radiation," Combustion and Flame, 11.

Stockstad, D.S. [1975], "Spontaneous and Piloted Ignition of Cheatgrass," draft of USDA Research Note.

REFERENCES (Concluded)

Tarifa, C. Sanchez [1965], "On the Flight Paths and Lifetimes of Burning Particles in Wood," Tenth Symposium on Combustion, 1964, The Combustion Institute, pp. 1021-1037.

Tarifa, C. Sanchez [1967], "Transport and Combustion of Firebrands," U.S. Department of Agriculture, Madrid University Report, 90 pp.

Thomas, P.H. [1963], "The Size of Flames from Natural Fires," Ninth Symposium on Combustion, 1962, The Combustion Institute.

Thomas, P.H., R. Baldwin and A.J.M. Heselden [1965], "Buoyant Diffusion Flames: Some Measurements of Air Entrainment, Heat Transfer, and Flame Merging," Tenth Symposium on Combustion, 1964, The Combustion Institute.

Young, P.H. [1973], "Firebrand Trajectory Model," Report No. ATR-74 (8158)-1, The Aerospace Corporation, El Segundo, California, 16 pp.

AEROSPACE CORPORATION

INTERNAL DISTRIBUTION LIST

(REFERENCE: COMPANY PRACTICE 7-21-1)

REPORT TITLE

STATISTICAL MODEL FOR SPOT FIRE HAZARD

REPORT NO.	PUBLICATION DATE	SECURITY CLASSIFICATION
ATR-77(7588)-1	20 December 1976	Unclassified

(NOTE: FOR OFF-SITE PERSONNEL, SHOW LOCATION SYMBOL, e.g. JOHN Q. PUBLIC/VAFB)

E. B. Anderson (3)
J. B. Fedele (6)
E. G. Hertler
S. D. Huffman
R. H. C. Lee
A. Muraszew (6)
T. D. Taylor
J. Vasiliu

APPROVED BY J. Stevens DATE 1/27/77

SHEET 1 OF 1

THE AEROSPACE CORPORATION

EXTERNAL DISTRIBUTION LIST

(REFERENCE: COMPANY PRACTICE 7-21-1)

REPORT TITLE

STATISTICAL MODEL FOR SPOT FIRE HAZARD

REPORT NO.	PUBLICATION DATE	SECURITY CLASSIFICATION
ATR-77(7588)-1	20 December 1976	Unclassified

MILITARY AND GOVERNMENT OFFICES	ASSOCIATE CONTRACTORS AND OTHERS

(NOTE: SHOW FULL MAILING ADDRESS; INCLUDE ZIP CODE, MILITARY OFFICE SYMBOL, AND "ATTENTION" LINE.)

Craig C. Chandler, Director
Division of Forest Fire and Atmospheric Sciences Research
USDA Forest Service
Washington, D. C. 20250

Stan Hirsch
Rocky Mountain Range and Experiment Station
240 West Prospect
Fort Collins, Colorado 80521

James E. Kerr, Staff Director
Support Systems Research
Disaster Preparedness Agency
Washington, D. C. 20301

Dr. Charles W. Philpot
Riverside Forest Fire Laboratory
P. O. Box 5007
Riverside, California 92507

Richard C. Rothermel (3)
Research Project Leader
USDA Forest Service
Intermountain Forest and Range Experiment Station
Northern Forest Fire Laboratory
Drawer G
Missoula, Montana 59801

Press Butler
Stanford Research Institute
333 Ravenswood Avenue
Menlo Park, California 94025

G. M. Byram
5 Cherry Lane
Asheville, North Carolina 28804

Professor Howard E. Emmons
California Institute of Technology
Mail Stop 301-46
Pasadena, California 91109

Frank Fendell
TRW, Inc.
Building R1, Room 1016
One Space Park
Redondo Beach, California 90278

Professor Melvyn Gerstein
Associate Dean, Graduate Affairs
School of Engineering
University of Southern California
University Park
Los Angeles, California 90007

☐ THIS DISTRIBUTION LIST PERMITS ONLY PRIMARY DISTRIBUTION OF THIS TOR.

AFR 80-45 DISTRIBUTION STATEMENT X'D BELOW APPLIES

☐ NO DISTRIBUTION STATEMENT
(Classified documents only)

☐ A. APPROVED FOR PUBLIC RELEASE; DISTRIBUTION UNLIMITED

☐ B. DISTRIBUTION LIMITED TO U. S. GOV'T AGENCIES ONLY;
_____;
(Reason)
_____. OTHER REQUESTS FOR THIS DOCUMENT
(Date statement applied)
MUST BE REFERRED TO _____.
(Controlling DOD office)

APPROVED BY _____ DATE 1/27/77
(FOR THE AEROSPACE CORPORATION)

APPROVED BY _____ _____ DATE _____
(FOR COGNIZANT AF OFFICE) (SYMBOL)

IF LIST COMPRISES TWO OR MORE SHEETS, COMPLETE THIS SIGNATURE BLOCK ON LAST SHEET ONLY

SHEET 1 OF 2

AEROSPACE FORM 2380 REV 7-75

THE AEROSPACE CORPORATION

EXTERNAL DISTRIBUTION LIST

(REFERENCE: COMPANY PRACTICE 7-21-1)

REPORT TITLE

STATISTICAL MODEL FOR SPOT FIRE HAZARD

REPORT NO.	PUBLICATION DATE	SECURITY CLASSIFICATION
ATR-77(7588)-1	20 December 1976	Unclassified

MILITARY AND GOVERNMENT OFFICES	ASSOCIATE CONTRACTORS AND OTHERS

(NOTE: SHOW FULL MAILING ADDRESS; INCLUDE ZIP CODE, MILITARY OFFICE SYMBOL, AND "ATTENTION" LINE.)

Richard Chase (50)
Riverside Forest Fire Laboratory
P.O. Box 5007
Riverside, California 92507

Andrew Stein
Riverside Forest Fire Laboratory
P.O. Box 5007
Riverside, California 92507

Dr. William C. Kuby
Mechanical Engineering Department
University of California - Santa Barbara
Santa Barbara, California 93106

Professor S. L. Lee
State University of New York at Stony Brook
Stony Brook, New York 11790

Peter H. Kourtz, Research Officer
Forest Fire Research Institute
Canadian Forestry Service
Ottawa, Canada

R. E. Martin
College of Forestry Resources
University of Washington
Seattle, Washington 98195

Dr. William G. O'Regan
Forest Service
P.O. Box 245
Berkeley, California 94701

Dr. P. P. Pagni
College of Engineering
University of California at Berkeley
Berkeley, California 94720

☐ THIS DISTRIBUTION LIST PERMITS ONLY PRIMARY DISTRIBUTION OF THIS TOR.

AFR 80-45 DISTRIBUTION STATEMENT X'D BELOW APPLIES

☐ NO DISTRIBUTION STATEMENT
(Classified documents only)

☐ A. APPROVED FOR PUBLIC RELEASE; DISTRIBUTION UNLIMITED

☐ B. DISTRIBUTION LIMITED TO U. S. GOV'T AGENCIES ONLY; _____ ; (Reason)
_____ . OTHER REQUESTS FOR THIS DOCUMENT (Date statement applied)
MUST BE REFERRED TO _____ . (Controlling DOD office)

APPROVED BY D. L. Stevens (FOR THE AEROSPACE CORPORATION) DATE 1/27/77

APPROVED BY _____ (FOR COGNIZANT AF OFFICE) _____ (SYMBOL) DATE _____

IF LIST COMPRISES TWO OR MORE SHEETS, COMPLETE THIS SIGNATURE BLOCK ON LAST SHEET ONLY

SHEET 2 OF 2

AEROSPACE FORM 2380 REV 7-75